

Spherical Multiple-Cell Grid and Applications in Ocean Surface Wave Models

Jian-Guo Li*

Met Office, Exeter EX1 3PB, United Kingdom

28 Mar 2024

Abstract: The spherical multiple-cell (SMC) grid is an unstructured latitude-longitude (lat-lon) grid, supporting flexible domain shapes and multi-resolution in desired areas. It retains the quadrilateral cells as in the standard lat-lon grid so that the simple finite difference schemes could be used. Sub-time-steps are applied on different cell sizes to speed up propagation calculations with a choice of 2nd or 3rd order advection schemes. Grid cells are merged at high latitudes to relax the CFL restriction and a fixed reference direction is used to define wave spectra in the polar region so that the SMC grid can be extended to the full globe, including the whole Arctic. The multi-resolution refinement is useful to resolve small islands and coastline details, which are important in ocean surface wave propagations. The SMC grid has been implemented in the WAVEWATCH III community wave model since 2012 and updated in the latest public release WW3 V6.07. A SMC 3-6-12-25 km multi-resolution global wave forecasting model has been used operationally in the UK Met Office since October 2016, leading to great reduction of model errors in comparison with our old 35km model and other global wave forecasting systems in the world. The SMC grid can also be applied on a rotated lat-lon grid for high latitude regions and this will be illustrated with a UK regional model at 1.5-3 km resolutions and an Arctic model at 1/16-1/8-1/4° spatial resolutions. Multi-grid option in WW3 is also extended to SMC grid and it allows same ranked SMC sub-grids to run in parallel on modern supercomputers, greatly expanded the use of computing resources in combination with the MPI-OpenMP hybrid parallelization. This guide will outline the underlying numerical techniques for the SMC grid and applications in ocean surface wave models, particularly for the latest V6.07 public release and some new updates for the future Vn7 public release.

Contents

- 1. Introduction
- 2. Wave propagation on a sphere
- 3. The SMC grid and numerical schemes
 - 3.1. SMC grid cell and face arrays
 - 3.2. Advection-diffusion schemes
 - 3.3. Refraction and spectral shift schemes
 - 3.4. The polar problem
 - 3.5. Spatial gradient and point mapping subroutines
- 4. Input/Output for SMC option
- 5. SMC grid propagation test
- 6. Applications of SMC grids in the UK Met Office
- 7. Applications of SMC grids around the world
- 8. Summaries and references

Corresponding author address: Dr Jian-Guo Li, Met Office, FitzRoy Road, Exeter EX1 3PB, UK
Email: Jian-Guo.Li@metoffice.gov.uk Tel. +44 33013 50548.

1. Introduction

The ice edge in the Arctic is retreating at unexpected speeds in recent years and reached as high as 86° N in summer 2007 and almost at the North Pole in 2012, opening shipping routes across the Arctic and calling ocean surface wave models to extend at high latitudes. The major problem to extend a latitude-longitude (lat-lon) grid wave model at high latitudes is the diminishing longitude grid-length towards the Pole, which exerts a severe restriction on time steps of finite-difference schemes (advection and diffusion in particular). Another problem is the increased curvature of the parallels at high latitudes. The rapid change of the local east direction renders the scalar assumption invalid for any vector component defined relative to the local east direction. The spherical multiple-cell (SMC) grid has been developed to tackle the polar problems (Li 2011). It relaxes the Courant-Friedrichs-Lowy (CFL) restriction of the Eulerian advection time-step by merging longitudinal cells towards the Poles as in the reduced grid (Rasch 1994). Round polar cells are introduced to remove the polar singularity of the spherical coordinate system. Vector component propagation errors caused by the scalar assumption at high latitude is removed by replacing the local east with a fixed reference direction, for instance, the map-east as viewed in a polar stereographic projection.

Besides, the SMC grid has the flexibility to remove all land points out of the wave propagation schemes and requires minimal changes to the lat-lon grid finite-difference schemes because the lat-lon “rectangular” cells are retained. Unresolved small islands incur errors in global ocean surface wave models as they are important sinks of the ocean surface wave energy (Tolman 2003). Missed island groups in coarse resolution global models lead to a persistent under-prediction of wave energy blocking. Although the far field errors can be alleviated with sub-grid obstructions, using high resolution cells is still the most appropriate approach for accurate swell prediction close to islands (Chawla and Tolman 2008). One feature of the unstructured SMC grid is that it can handle multiple resolutions within the same model, so that small islands and coastlines are resolved at high resolutions while the vast open oceans are kept at an affordable resolution. This is a very appealing option for operational models as increasing resolution throughout the full model domain to resolve small islands is not economical. The multi-resolution feature of the SMC grid also allows regional models to be merged into one global model, another desirable advance in future operational wave modelling.

With the advances of super computers, more computing resources are available for wave forecasting models but the WW3 model has a hard limit of computing core usage due to its built-in spectral parallelisation scheme. Hybrid parallelization is one way to extend the WW3 computing core usage and multi-grid mode is another way to run several grids in parallel. The SMC grid package in WW3 has extended for hybrid parallelization in the last public release and multi-grid option is added recently to further expand its computing core usage for next generation supercomputers.

The SMC grid was implemented in the WAVEWATCH III® wave model (WW3, Tolman 1991; Tolman et al 2002) in the 2012 V4.18 public release and updated in the subsequent V5.16 and V6.07 public releases (WW3DG 2019). Scalar advection schemes on the SMC grid are described in Li (2011) and ocean surface wave propagation on a SMC grid is presented in Li (2012). Details of the map-east method for the Arctic part in the SMC grid are given in Li (2016). This guide summarises the underlying numerical techniques for the SMC grid and essential steps to build a SMC grid, particularly how to configure a SMC grid in the WW3. Applications of SMC grids in operational wave forecasting and researches so far around the world are also described, particularly in the UK Met Office.

2. Wave propagation on a sphere

The Eulerian ocean surface wave model is based on a 2D spectral energy balance equation. In the 2-D spherical coordinates with longitude λ and latitude φ , the equation is given by

$$\begin{aligned} \frac{\partial \psi}{\partial t} + \frac{\partial F_x}{\partial x} + \frac{\partial(F_y \cos \varphi)}{\cos \varphi \partial y} + \frac{\partial(k\psi)}{\partial k} + \frac{\partial(\theta\psi)}{\partial \theta} &= S \\ F_x &\equiv u\psi - D_x \frac{\partial \psi}{\partial x} \\ F_y &\equiv v\psi - D_y \frac{\partial \psi}{\partial y} \end{aligned} \tag{1}$$

where $\psi(t, \lambda, \varphi, k, \theta)$ is any component of the wave energy spectrum, t is the time, k is the wave number, θ is the spectral direction usually defined from the local east direction, u and v are the zonal and meridian components of the wave energy propagation speed, D_x and D_y are the diffusion coefficients, and S the source term. The geophysical coordinates x and y are defined locally eastward along the parallel and northward along the meridian, respectively. So their spatial increments are given by $dx = r\cos\varphi d\lambda$, $dy = rd\varphi$, where r is the radius of the sphere. The overhead dot indicates time differentiation along the wave propagation path. The r.h.s S represents all source terms and they are unchanged from the original WW3 model. Note that in WW3 model the wave action $A \equiv \psi/\omega$, where ω is the intrinsic angular frequency of the ocean surface wave, is chosen instead of the wave energy ψ for conservation when ocean current is present. The wave action shares the same equation (1) as the wave energy except that the source term is divided by ω . Hence all propagation schemes for wave energy can be applied on wave action.

The spherical wave energy balance equation (1) differs from its Cartesian counterpart in the meridian differential term by an extra cosine factor, which renders the term undefined (singular) at the Poles. Thus, except for at the Poles, Eq. (1) can be approximated with finite-difference schemes similar to those used in the Cartesian grid. The only difference between the Cartesian and spherical versions of these finite-difference schemes is that the latter has an extra cosine factor. Because the SMC grid retains the lat-lon grid cells, the wave energy balance equation (1) is also valid on the SMC grid.

The diffusion term in (1) may be considered as the sub-grid mixing term because the model wave spectrum represents the spatial average over one grid cell. This diffusion term is usually parameterised to alleviate the so-called garden-sprinkler effect (GSE) due to discretization of the wave energy spectrum (Booij and Holthuijsen 1987, Tolman 2002).

One primary physical process that affects surface wave propagation is the depth-induced refraction. Refraction formulations in contemporary surface wave models are based on the linear wave theory, assuming slow-varying ocean depth. The refraction on the SMC grid follows the same formulations in the WW3 (Tolman 1991):

$$\dot{k} = -\xi \mathbf{k} \cdot \nabla h - \mathbf{k} \cdot \nabla U_k \quad (2a)$$

$$\dot{\theta}_{rfr} = -\xi \mathbf{n} \cdot \nabla h - \mathbf{n} \cdot \nabla U_k \quad (2b)$$

where $\mathbf{k} = (k\cos\theta, k\sin\theta)$ is the wave number vector, h is the water depth, ∇ is the 2-D gradient operator, U_k is the ambient current velocity component along the \mathbf{k} direction, $\xi = \omega/\sinh(2kh)$ will be referred to as the *refraction factor* and and $\mathbf{n} = (-\sin\theta, \cos\theta)$ is a unit vector normal to the \mathbf{k} direction to the left or at $\theta + \pi/2$. The wave number change rate (2a) is also known as the spectral shift and the direction change rate (2b) is called the refraction rate. More details on derivation of these refraction rates are available in Li (2012).

Wave energy travels along the shortest route on the ocean surface, that is, along great circles on the sphere. So a wave spectral component will not be confined at its defined direction but will shift gradually with latitude along its great circle path, a procedure known as great circle turning (GCT). Assuming the great circle direction is at an angle θ from the local east direction at latitude φ , the product of cosines of these two angles is conserved on the great circle path, that is, $\cos\theta\cos\varphi = const.$, which provides a simple rule for navigation along great circles and leads to the following GCT rate along the propagation direction

$$\dot{\theta}_{gct} = -(c_g/r)\cos\theta\tan\varphi \quad (3)$$

where c_g is the wave group speed defined by

$$c_g = c_{gd} \left(\tanh(kh) + kh/\cosh^2(kh) \right) \quad (4)$$

in which $c_{gd} = g/2\omega$ is the group speed in deep waters. The net wave direction changing rate used in (1) for the SMC grid is then the sum of the refraction rate (2b) and the GCT rate (3).

3. The SMC grid and numerical schemes

Scalar advection schemes on the SMC grid are described in Li (2011). Here summarised are other terms in (1) and treatment of advection and diffusion on the multi-resolution SMC grid. It also tackles the polar problem with vector components at high latitudes.

3.1. SMC grid cell and face arrays

A global SMC grid is shown in Fig.1. For clarity, only the European and Arctic regions are shown here. The base resolution of the SMC grid is set to be $\Delta\lambda = 360^\circ/1024 = 0.3515625^\circ$ and $\Delta\varphi = 180^\circ/768 = 0.234375^\circ$ such that the latitudinal grid length is about 25 km. The SMC grid uses only the sea points or cells and refines model resolution (by two levels) down to about 6 km around islands and near coastlines, results in a global 3-level (6-12-25 km) SMC grid on the global ocean surface. This SMC grid will be referred to as the SMC6-25 grid. Cells are merged longitudinally at high latitudes following the same rules in Li (2011) to relax the CFL restriction. A unique 5-element integer array is assigned to each cell to hold its SW corner x -, y -indices (i, j), cell x -, y -sizes ($\Delta i, \Delta j$), and water depth (h), as illustrated in Fig.2. The x - and y -indices are measured in size-1 cell increment so the cell centre latitude and longitude can be worked out with

$$\varphi_j = \varphi_0 + (j + 0.5 * \Delta j) \Delta\varphi; \quad \lambda_i = \lambda_0 + (i + 0.5 * \Delta i) \Delta\lambda \quad (5)$$

where λ_0 and φ_0 are the origin of the cell x - and y -indices. For the SMC6-25 grid, the origin of the grid indices is set at zero-meridian on the Equator so both λ_0 and φ_0 are zero. The mapping rule (1) is exactly the same as that for the lat-lon grid cells except for that the SMC grid cells are not arranged in spatial sequence (hence is called an unstructured grid) and their sizes may change by a multiple of 2 (size-1, size-2, size-4, ...). The depth h is also rounded to an integer so the whole cell array can be declared as an integer array. The cells are listed as a 1-D array and sorted by their y -size for use of sub-time steps on refined cells. Please note that the sorting is on the y -size not the x -size because the cell x -size may change on the same resolution level due to the longitudinal merging at high latitudes. The cell y -size will be in ascending order in the sorted cell array list and the number of cells for each resolution level (of a given y -size) is listed on the first line of the cell array file after the total cell number. This cell number counts will be used for declaring the cell array variable and setting the sub-loops for propagation schemes.

It should be emphasized that the cell size must be increased no more than one level for any neighbouring cells, that is, around a size-1 cell the neighbouring cells can be either size-1 or size-2. Similarly, size-2 cells can be linked to cells of the same size-2 or either one level down (size-1) or one level up (size-4). This one level size change rule ensures resolution varies gradually and simplifies the face flux formulation. Putting cells of more than one level size differences side by side would jeopardise the present face array generating program.

Once the cell arrays are compiled in sorted order, cell face arrays can be generated with an extra FORTRAN program. Cell faces are named by its normal velocity components as u - or v -faces. A 7-element integer array is pre-calculated for each face to store its face position, size and its upstream-central-downstream (UCD) cell indices. An extra y -size integer is added for the v -face array for sorting purposes. Face sizes are chosen to be the minimum size between the two neighbouring cells. For a cell face neighbouring two cells of one level below, the face is divided into two faces of the lowered level size. This minimised face size ensures one face links two cells only. The face arrays are also sorted by its y -size so that the multi-resolution advection/diffusion loops can be divided into multi-step sub-loops. The total face number and sub-level face numbers are listed on the first line of the face array file for propagation and mapping purposes. The face arrays are used to calculate the advection-diffusion and the depth gradient.

For the multi-resolution SMC6-25 grid, the face and cell loops are sorted into 3 sub-loops by their y -sizes, thanks to the unstructured nature of the SMC grid. Advection-diffusion terms for the refined 6- and 12-km cells are calculated at $\frac{1}{4}$ and $\frac{1}{2}$ of the base level time step, that is, the 6-km flux and cell loops are done twice before the 12-km flux and cell loops are calculated once. The base level

flux and cell loops are only calculated at each base level time step. A temporary net-flux variable is used to accumulate fluxes between different levels and is reset to zero once it is used for its cell update. The simple loop-regrouping technique for multi-resolution SMC grid allows a smooth transfer from a single resolution SMC grid to a multi-resolution grid with optimised efficiency.

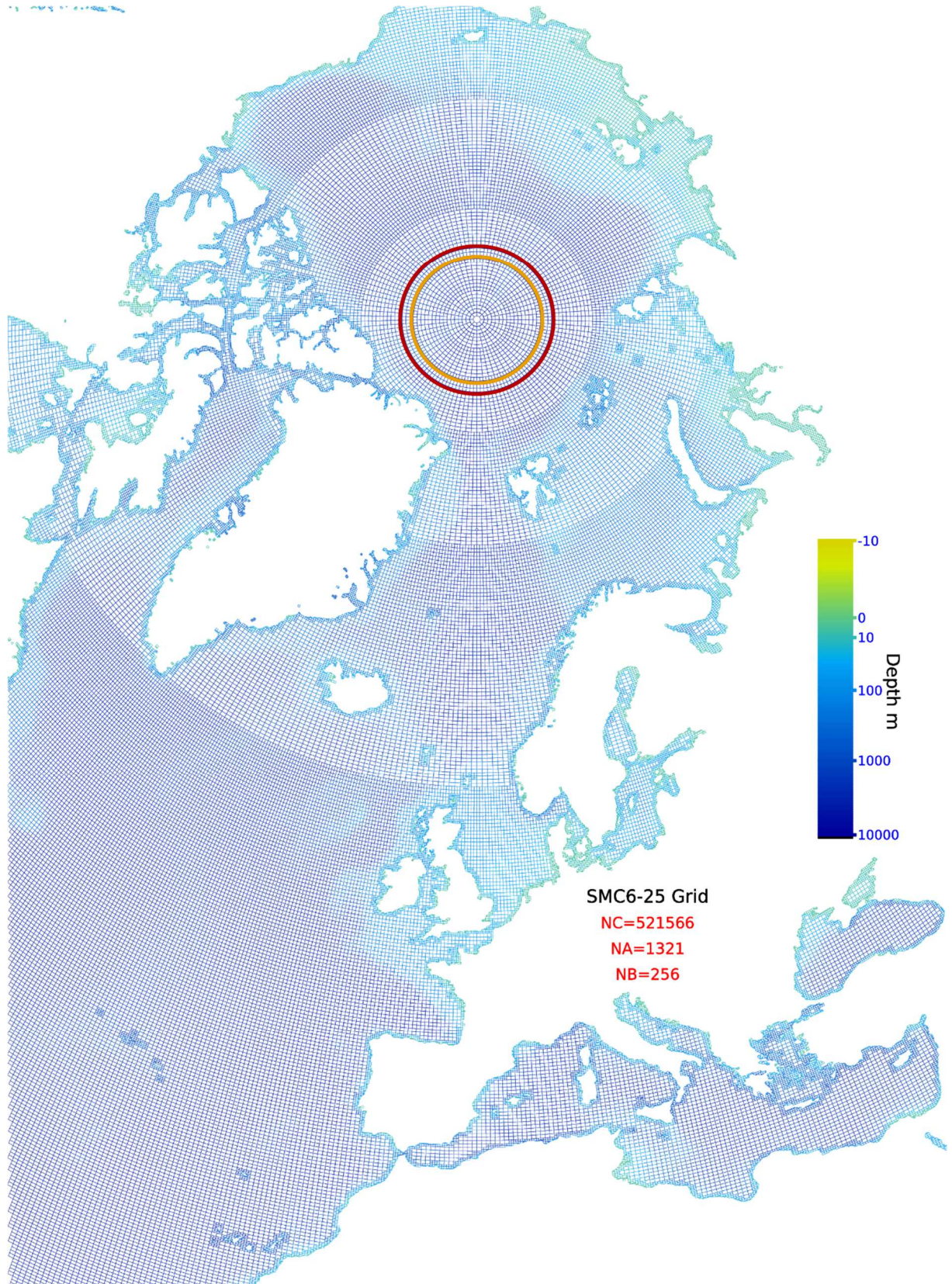


Fig.1. The European and Arctic regions of the SMC6-25 grid.

For refinement interface, such as a cell face between a coarse and two refined cells, SMC grid assumes a first order approximation that the coarse cell is uniform within its cell area and it could be divided into two halved cells of the same properties as the coarse cell. This approximation avoids interpolations between different sized cells, whose centres are unaligned due to the halved refinement. The dashed green lines in Fig.2 indicate how the coarse cells marked by the solid red lines are divided into halved cells. The green dots indicate the centres of those halved virtual cells, which are aligned with the refined cells. Finite difference across such a refinement interface is then approximated by averaged differences between the halved cells and the refined cells. Propagation face fluxes are calculated on refined faces at refinement interface. These refined fluxes are automatically averaged for coarse cells in their net fluxes. Spatial gradients between different sized cells are also averaged in this way for coarse cells. So for a coarse cell bounded by a coarse cell on the left and two refined cells on the right, its cell gradient will be the average of one face gradient between the coarse cells and two refined face gradients between the halved virtual cells and the two refined cells. This is equivalent to a space-centred gradient scheme except that across the refinement interface the averaged difference is used. This average may partially remove short waves or noises caused by the refinement. This approximation on refinement interface is used for all spatial schemes, including advection, diffusion, average and gradient schemes on the SMC grid.

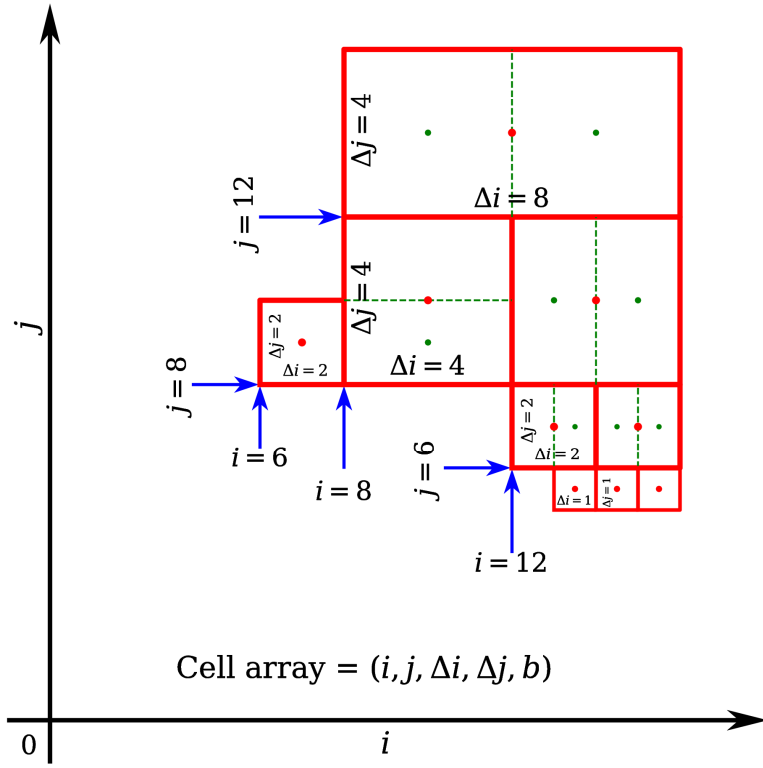


Fig.2. Illustration of SMC grid cell arrays.

3.2. Advection-diffusion schemes

The l.h.s terms in (1) are calculated with time-splitting approaches by combining the first (time differential) term with each of the other 4 terms. The advection-diffusion terms are discretised on the SMC grid with one flux loop and one cell loop for each dimension. Note that the diffusion term used here is slightly different from the original GSE smoothing term (Booij and Holthuijsen 1987). The original diffusion term is designed to enhance the transverse smoothing because a first order upstream advection scheme is used, and it has already introduced strong smoothing along the wave propagation direction. The asymmetrical diffusion results in a cross term in Cartesian coordinates. In this SMC grid wave model, the advection is estimated with an upstream non-oscillatory 2nd order (UNO2) scheme (Li 2008), which is adapted from the MINMOD scheme (Roe 1985). As the implicit diffusion of the 2nd order advection scheme is much smaller than that of the first order scheme, the diffusion

term is simplified to be isotropic, so the cross-term vanishes. Besides, the refraction and GCT term provides extra directional smoothing, which makes the total smoothing biased towards the transverse direction, close to the original asymmetrical smoothing term.

The isotropic diffusion coefficient is defined in WW3 by $\kappa = (c_g \Delta\theta)^2 T_s / 12$, where c_g is the wave component group speed, $\Delta\theta$ is the directional bin width and T_s the swell age. To avoid instable diffusion, the swell age is tuned so that the diffusion Fourier number is less than $1/2$. A guide rule for the maximum swell age T_s is given by

$$T_s \leq \frac{6}{\Delta t_a} \left(\frac{\Delta x_0}{c_{gm} \Delta\theta} \right)^2 \quad (6)$$

in which Δt_a is the advection time step, Δx_0 is the base level grid length on the Equator, $\Delta\theta$ is the directional bin width (in radian) and c_{gm} is the maximum group speed in the model spectral range (usually at the lowest frequency end). Note that the advection time step is adjusted to ensure the Courant number $c_{gm} \Delta t_a / \Delta x_0 < 1$, the expression (6) may be simplified as $T_s \leq 6 \Delta x_0 / (c_{gm} \Delta\theta^2)$. If the swell age is set too large, the diffusion term will become unstable and eventually bring the model to a crash. It would be convenient if the swell age was reduced automatically inside the model when users accidentally set it too large. This automatic adjustment, however, has not been set up yet. If the diffusion term is not enough to smooth out the garden sprinkler effect, an additional 1-2-1 weighted smoothing term is also available by defining the PSMC namelist variable AVERG in the `ww3_grid.inp` file. This averaging is equivalent to the diffusion term with a Fourier number of $1/4$.

The advection flux with the UNO2 scheme and the diffusion flux with a central-space finite difference scheme for a u -face between the central and downstream cells are merged into a single flux, given by

$$\Delta F_x = (u \psi^* - D_x G_{DC}) l_u \Delta t \quad (7)$$

where ψ^* is the mid-flux value evaluated with the UNO2 scheme (see Eq. (6) in Li 2008), $G_{DC} = (\psi_D - \psi_C)/(x_D - x_C)$ is the gradient between the central and downstream cells, l_u is the u -face length and Δt is the sub-time step. Both the advection and diffusion schemes are of 2nd order accuracy. The diffusion coefficient, $D_x = D_y$, is specified by the spectral component propagation speed, directional bin width and a user input swell age parameter as the transverse diffusion coefficient D_{nn} in the original model. In the presence of an ambient ocean current, the wave energy propagation speed in the x -direction should be the sum of the group speed and current speed components, that is, $u = c_g \cos\theta + U_x$.

A temporary net-flux variable, F_{net} , is used for each cell to gather all fluxes into the cell before it is used for the cell value update. The flux (7) is added to the downstream cell net-flux variable and subtracted from the central cell net-flux variable at the same time for energy conservation. The use of face sizes and the net flux variables allow fluxes from different sized faces to be added up in proportion to their face sizes. After the face loop is completed, each cell value is updated in a cell loop by

$$\psi^{n+1} = \psi^n + F_{net} / (l_x l_y) \quad (8)$$

where $l_{x/y}$ is the cell x/y -length. The cell y -length is required for x -flux update to cancel the face length used in sum of the fluxes in proportion to the u -face length. The v -face fluxes are calculated similarly except for the additional latitude cosine factor.

For the multi-resolution SMC6-25 grid, the face and cell loops are sorted into 3 sub-loops according to their y -sizes, thanks to the unstructured nature of the SMC grid. Advection-diffusion terms for the refined 6- and 12-km cells are calculated at $1/4$ and $1/2$ of the base level time step, that is, the 6-km flux and cell loops are done twice before the 12-km flux and cell loops are calculated once. The base level flux and cell loops are only calculated at each base level time step. The temporary net-flux variable is used to accumulate fluxes between different levels and is reset to zero once it is used for its cell update. The simple loop-regrouping technique for multi-resolution SMC grid allows a

smooth transfer from a single resolution SMC grid to a multi-resolution grid with optimised efficiency.

Another feature of the SMC grid is the unification of boundary conditions with internal flux evaluations. Cell faces at coastlines are assumed to be bounded by two consecutive empty cells when the face arrays are generated. Thus, any wave energy transported into these empty cells will disappear, and no wave energy will be injected out of these zero cells into any sea cells. This convenient setup conforms to the zero-wave energy boundary condition at land points used by ocean surface wave models and allows all the boundary cell faces to be treated in the same way as internal faces in one face loop. In addition, the periodic boundary condition for a global model is automatically included by the unstructured grid. So short boundary loops are avoided in the SMC grid propagation schemes and the full face and cell loops are streamlined for vectorization and parallelization.

An additional benefit of using two consecutive zero-boundary cells beyond the coastline is the complete blocking of wave energy by single-point islands. On a conventional lat-lon grid, wave energy can ‘leak’ through a single-point island due to the interpolation with neighbouring sea points in transport schemes when a 5-point stencil is used. In the SMC grid, the default UNO2 scheme (Li 2008) and an optional 3rd order UNO3 scheme are also based on 5-point stencil but any single-point island is extended with two zero cells beyond its boundary face, thanks to the unstructured feature. As a result, wave energy cannot pass through such ‘expanded island’. Nevertheless, the sub-grid obstruction scheme from the original WAVEWATCH III model is kept to account for islands unresolved by the highest resolution cells. The sub-grid obstruction scheme follows the approach of Hardy et al (2000) with some modifications (Tolman 2003).

From the WW3 V5.16 onwards, an optional 3rd order advection UNO3 scheme (Li 2008) is added so users may replace the default UNO2 scheme with the UNO3 scheme by defining a namelist (`PSMC`) variable `UNO3` in the `ww3_grid.inp` file. The UNO3 scheme is equivalent to the Ultimate Quickest (UQ) scheme (Leonard 1991, Leonard et al 1996) used for regular lat-lon grids but it replaces the UQ scheme’s flux limiters with the UNO2 scheme. In practice, it is enough to use the default UNO2 scheme, as the UNO3 option does not bring much improvement to wave model performance but adds about approximately 30% extra computation load. This is because the strong smoothing for controlling the garden sprinkler effect will degrade any high order advection scheme to an equivalent 1st order scheme. This is also true to regular grid models, where the 2nd order scheme (UNO option) allows sufficient freedom to choose directional bins and set diffusion parameters. The results are expected to be equivalent to those with the UQ option, whilst saving computing time.

3.3. Refraction and spectral shift schemes

It should be emphasized that the linear surface wave theory is only valid when the water depth is non-zero (Falnes 2002). When h approaches zero, for instance, the refraction rate (2b) becomes undefined because the ξ factor approaches infinity ($\xi \sim 0.5\sqrt{g/h}$). It is then customary in wave models to use a minimum water depth for the refraction term. A minimum water depth of 10 m is recommended, and the refraction factor will then be less than 0.5.

Apart from shallow water depth, steep ocean floor and large time step may also result in a large refraction rate. For instance, if the discrete depth gradient is assumed to be $\Delta h/\Delta x = 0.1$ and time step is $\Delta t = 1000$ s, the maximum refraction angle per time step might be $\Delta t \Delta h / 2 \Delta x \sim 50$ rad or about 8 full circles, which is no longer physically meaningful and is too large to fit into any advection-like refraction schemes used in contemporary wave models. One way to avoid this unrealistic large refraction increment is to use a small timestep but this usually turns out to be too restrictive for wave models. Since refraction in a wave model is usually a minor process and is confined to coastal regions, the refraction increment is simply reduced to fit for the advection-like CFL condition in some wave models (WAMDI group 1988, Booij et al 1999, Tolman et al 2002). The CFL condition requires the refraction angle increment per time step to be less than one directional bin width (about 10°) and, of course, reduces the refraction effect. The latest version of the WAVEWATCH III model uses sub-time step to relax this restriction on the refraction term.

Here for the SMC grid wave model, a rotation scheme is substituted for the advection-like scheme to estimate the refraction term so that the CFL limit can be avoided. The rotation scheme is similar to a re-mapping advection scheme and is unconditionally stable. Although the rotation scheme

does not have any limit on the refraction increment, the refraction angle should not pass beyond the depth gradient line (where $\mathbf{n} \cdot \nabla h = 0$) as stated in the refraction rate (2b). This physical limiter on the total refraction angle is included in the rotation scheme. The angle between the spectral direction and the depth decrease direction is calculated by:

$$\gamma = \cos^{-1} \left[- \left(h_x \cos \theta + h_y \sin \theta \right) / \sqrt{h_x^2 + h_y^2} \right] \quad (9)$$

where h_x and h_y are the water depth gradient along x and y axis, respectively. Because FORTRAN function ACOS returns value between 0 and π , the maximum refraction angle (absolute value) is then chosen to be less than $\pi/2$ with $\Delta\theta_{mxfr} = \min(\eta, \gamma, \pi - \gamma)$. The constant η ($< \pi/2$) is a user-defined maximum refraction angle to reduce the refraction effect if required. If η is set to be less than one directional bin width, the rotation scheme will be equivalent to the original advection-like scheme in the WAVEWATCH III model without using sub-timesteps. For the present comparison study, the refraction limiter is set to be $\pi/3$. This refraction limiter may prevent all directional components from converging at the depth gradient direction within one timestep, which may result in unrealistic large wave energy like caustics in ray tracing models. It also creates room for merging the refraction with other directional changing terms, such as the refraction by ambient current and the GCT term.

The GCT term (3) can be fit into an advection-like scheme because it is usually less than one directional bin ($\sim 10^\circ$). For instance, if the time step is less than 900 s, the GCT angle (3) will be less than 1° per time step below 85° latitude, as the wave propagation angular speed, c_g/r , is on the order of 10^{-6} rad s $^{-1}$. However, as the refraction term is calculated with a rotation scheme in the SMC grid model, the GCT term is simply appended to the refraction term to form a total rotation angle. The rotation subroutine rotates each directional component by the combined angle and partitions its energy into the two directional bins which the rotated one strides across after the rotation. This simple rotation subroutine not only removes the time step restriction on the refraction angle but also adds an implicit diffusion in the θ direction because its implicit diffusivity is equivalent to that of the first order upstream scheme. This additional smoothing in the transverse direction is desirable for wave models to mitigate the GSE.

The spectral shift term, fourth in (1), could be calculated with an advection-like UNO2 scheme in the k -space because the spectral shift is usually small enough to meet the CFL condition. As the sea floor gradient induced spectral shift is considered in the wave number modification, so this term is no longer needed in WW3. The current induced spectral shift is calculated with an advection-like UNO2 scheme in k -space at the advection sub-time step for all cell spectra. It is, hence, subject to a user defined CFL limiter. There is a possible interaction between the current spectral shift and source terms, which may result in erroneous high waves in high current speed areas when running high resolution models. This interaction is not fully understood at present and the most effective way to remove the high waves has been to switch off the current induced spectral shift, or massively reduce the k-shift limit (e.g. to a value of 0.01) if such high wave pockets appear. This issue has been found for regular grid models as well, so is not thought to be specific to the SMC model propagation scheme. Notice that the current induced refraction rotation and extra propagation are still in effect even the spectral shift is switched off.

3.4. The polar problem

The ocean surface wave energy spectrum is usually defined as discrete directional components from a reference direction at the local east and each directional component is assumed to be a scalar in wave propagation. This scalar assumption has been taken for granted in finite difference schemes, such as, calculation of the local gradient, $G_{DC} = (\psi_D - \psi_C)/(x_D - x_C)$, where the vector components ψ_D and ψ_C for the two neighbouring cells are assumed to be at the same direction, that is, to be treated as a scalar. This scalar assumption is a good approximation for a global wave model when the ice-covered Arctic area is excluded. However, the scalar assumption becomes erroneous at high latitudes on a reduced grid since the change of direction over one grid-length grows too large to be ignored. For instance, in the SMC6-25 grid (see Fig.1) there are 8 cells immediately around the polar cell, the local east direction changes by 45° over one cell length. Fig.3 is a zoom-in figure for the polar cell and its neighbouring cells to illustrate the invalid scalar assumption for vector component based on local east

reference direction in the polar region. This invalid assumption prevents extension of ocean surface wave models at high latitudes. This problem can be avoided by switching to a fixed reference direction, for instance, the map-east direction as viewed on a stereographic projection of the polar region. Assuming the angle from the map-east to the local east is α , the wave spectral component for a given direction of angle θ from the local east will have an angle $\theta' = \theta + \alpha$ from the map-east. Its zonal and meridian group speed components are then given by

$$\begin{aligned} c_g \cos \theta &= c_g \cos(\theta' - \alpha) \\ c_g \sin \theta &= c_g \sin(\theta' - \alpha) \end{aligned} \quad (10)$$

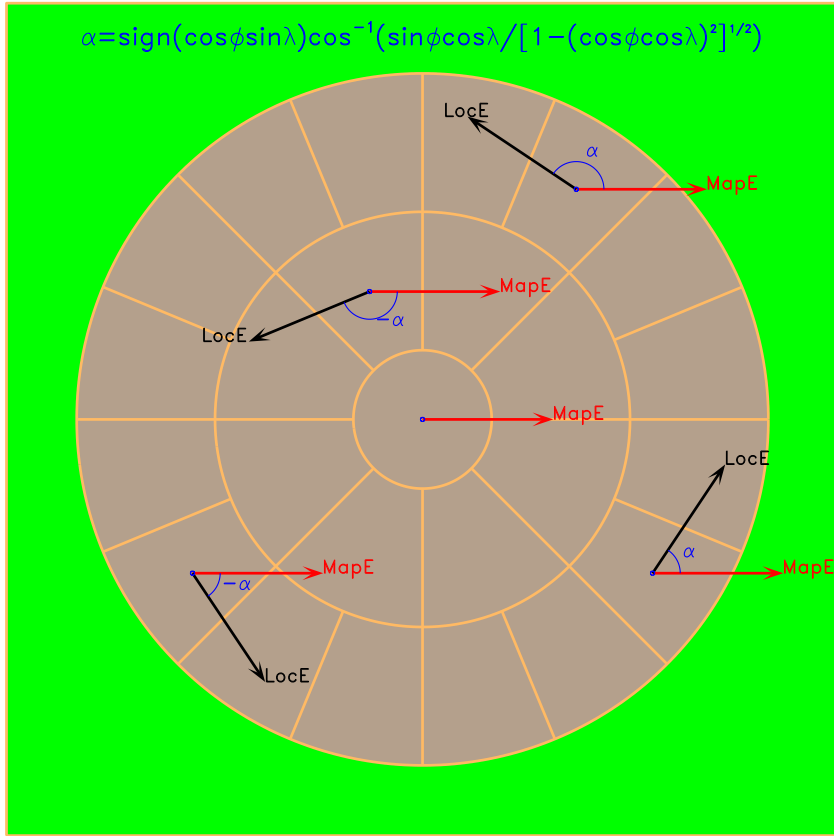


Fig.3. Relationship of local east and map-east reference direction systems.

Note that the polar cell does not have a local east direction so the velocity could not be defined at the Pole as zonal and meridian components. In the SMC grid, however, only the meridian velocity component at the edge of the polar cell is required and there is no need to define the velocity at the polar cell centre. This is one of the advantages of using a polar cell centred at the Pole. Nevertheless, velocity components at the Pole can be defined in the fixed reference system but they could not be converted into the local east system. Because a given direction θ' from the map-east is constant in the Arctic region, the spectral component in the map-east system can be treated as a scalar for transport in the polar region.

This map-east direction can be conveniently approximated with a rotated grid with its rotated pole on the Equator. The standard polar region becomes part of the ‘tropic region’ in the rotated grid so the longitudinal direction of the rotated grid can be substituted for the map-east direction. For instance, if the rotated pole is at 180°E on the Equator, the angle α from this map-east to the local east at longitude λ and latitude ϕ within the Arctic region can be worked out with:

$$\alpha = \text{sgn}(\cos \phi \sin \lambda) \arccos \left[\frac{\cos \lambda \sin \phi}{\sqrt{1 - (\cos \lambda \cos \phi)^2}} \right] \quad (11)$$

If the map-east is used within the Arctic region and local east in the rest for definition of the wave spectrum, there will be no fixed corresponding components between the two systems because the angle, α , between the local and map-east directions (10) varies with longitude and latitude as shown in Fig.3. For this reason, wave spectra defined from the map-east in the Arctic region could not be mixed up with the rest spectra defined from the local east reference direction. In the SMC grid shown in Fig.1, the reference direction change is set between the 3rd (at about 83°) and 4th (at 86.4°) size-changing parallels (see definition in Li 2011), where the local east direction changes less than 3° over one cell length as there are 128 cells in one row. The Arctic part and the rest (will be referred to as the *global part*) are linked together through 4 over-lapping rows. Wave spectra in the lower two of the 4 over-lapping rows in the Arctic part are updated with wave spectra from the global part after they are rotated anticlockwise by α . Wave spectra in the upper two rows of the 4 over-lapping rows in the global part are updated with wave spectra from the Arctic part after a clockwise rotation by α . Because of the unstructured nature of the SMC grid, the Arctic cells are appended behind the global part in the single cell list for propagation. The two parts can be conveniently separated by using sub-loops. The overlapping rows are treated in the same way as other cells, so the propagation is calculated together for both parts.

Wind direction and other direction related source terms must be modified within the Arctic part to use the map-east reference direction. If only the velocity components are dealt with within the Arctic (such as in a dynamic model), there is no need to work out the angle itself. The cosine and sine of the rotation angle will be enough for velocity conversion between the map-east and local east system. The rotation angle cosine and sine are given by

$$\cos \alpha = \frac{\cos \lambda \sin \varphi}{\sqrt{1 - (\cos \lambda \cos \varphi)^2}}, \quad \sin \alpha = \frac{\sin \lambda}{\sqrt{1 - (\cos \lambda \cos \varphi)^2}}, \quad (12)$$

The conversion between the map-east velocity components u' and v' and the local east velocity components u and v are given by

$$\begin{pmatrix} u' \\ v' \end{pmatrix} = \begin{pmatrix} \cos \alpha & -\sin \alpha \\ \sin \alpha & \cos \alpha \end{pmatrix} \begin{pmatrix} u \\ v \end{pmatrix}, \quad \begin{pmatrix} u \\ v \end{pmatrix} = \begin{pmatrix} \cos \alpha & \sin \alpha \\ -\sin \alpha & \cos \alpha \end{pmatrix} \begin{pmatrix} u' \\ v' \end{pmatrix} \quad (13)$$

That is, the local east velocity vector is rotated anticlockwise by the angle α as viewed in the map-east system. The wind component relationship (12) may also be used in the Arctic part to convert the local east wind to the map-east wind for wave model source terms.

The great circle turning (GCT) term (see Eq. 3) must be modified in the Arctic part to use the rotated grid latitude, which is close to zero in the Arctic part because the rotated Equator passes the North Pole. If the Arctic part is kept small around the polar region (like above 85°N in the SMC625 grid), this GCT term becomes negligible. The refraction term (see Eq. 2) retains the formulation in the Arctic part except for that the gradients of water depth and current component along the wave direction should be rotated to the map-east system. As the Arctic Ocean above 85°N is considered deep for wind waves, the refraction is also negligible in the small Arctic part.

3.5. Spatial gradient and point mapping subroutines

The spatial gradient of a given field variable at a sea point on a SMC grid may be required for other terms, such as wave scattering or bottom friction. The SMC grid module contains a convenient subroutine, `SMCGradn(HCel, GrHx, GrHy)`, which calculates the spatial gradients, `GrHx(1:NSEA)`, `GrHy(1:NSEA)`, of the given field `HCel(-9:NSEA)`. Note that the input field is extended from the normal range (1:NSEA) to (-9:NSEA) for the SMC grid. The `HCel(-9:0)` should be assigned the boundary values (on land points) used for this given field. For water depth as an example, set `HCel(-9:0)=0`. See the subroutine `SMCDHXY` in `f77/w3psmcmd.f77` for a calling example of this gradient subroutine. The spatial gradient will be in the map-east direction system for the Arctic part while in the local east system for the global part.

Two mapping subroutines, W3SMCELL and W3SMCGMP, are also added to the SMC grid module (ftn/w3psmcnd.ftn) to facilitate the multi-grid option in WW3, the W3SMCELL

```
SUBROUTINE W3SMCELL( IMOD, NC, IDC1, XLon, YLat )
```

will finds out the cell centre longitude and latitude for the NC cells listed by its cell array sequential number or IDC1(NC) in grid IMOD and return them by XLON(NC) and YLAT(NC). The W3SMCMAP

```
SUBROUTINE W3SMCGMP( IMOD, NC, XLon, YLat, IDC1 )
```

will find out whether the listed NC points specified by XLON(NC) and YLAT(NC) are inside the IMOD grid cells. It returns the cell IDs if any point is found in one cell; Otherwise, returns 0 cell ID in IDC1(NC). Note that the returned cell ID only tells the point is within the cell area but does not specify where it is inside the cell. The mapping accuracy at the SMC grid resolution is good enough as these two subroutines are used to find out boundary points in SMC sub-grids for the WW3 multi-grid option and the sub-grids are assumed to share identical boundary cells. For sub-grids which do not share identical boundary cells or in different grid types, the mapping may need some refinement. The multi-grid option for equal ranked SMC sub-grids will be available in WW3 Vn7.

4. Input/output files for SMC option

The regular lat/lon grid WW3 wave model requires input files for wind forcing, sea-ice coverage, water depth, sub-grid obstruction and land-sea masking. For SMC grid these regular grid input files are no longer required and they are replaced with sea-point only files. The water depth is stored in the last column of the cell array file in unit of meter. If the accuracy at a metre is not enough, users may use other units (such as cm) and convert the depth integer back to unit of metre inside the ww3_grid program. Using integer to represent water depth in the cell array is to ensure the cell array is completely an integer array. A corresponding regular grid at the base level resolution of the SMC grid is used to set up the WW3 model for the SMC grid option. For example, a 25km regular lat-lon global grid is used for setting up the input files for the SMC6-25 grid.

When compiling the WW3 executables, SMC switch should be added in addition to the regular lat/lon grid propagation switches PR3 UQ (as default) or PR2 UNO. The executables will work for either a regular grid or a SMC grid, depending on which grid type is specified in `ww3_grid.inp`. Most of the WW3 model will work the same way on either regular or SMC grid except for the propagation (advection, diffusion, refraction, and GCT), which will be calculated with the SMC module for a SMC grid. Extra input files for the SMC grid are required in the `ww3_grid` program. These extra input files include the SMC grid cell and face arrays and the modified cell-only sub-grid obstruction file. If input boundary condition is required for a regional model on a SMC grid, an extra boundary cell file is also required. If the Arctic part is included, it requires extra cell and face arrays for the Arctic part as well. These Arctic part cell and face arrays will be merged with the global part cell and face arrays inside the `ww3_grid` program so that propagation on the whole global grid is calculated within one loop.

In the `ww3_grid.inp` file a namelist PSMC is added for input of some SMC grid related parameters. The variables in the PSMC namelist are defined as

```
NAMELIST /PSMC/ CFLSM, DTIMS, RFMAXD, Arctic, AVERG, UNO3, &
          LvSMC, ISHFT, JEQT, NBISMIC, SEAWND
```

and they take the following default/initial values in `ww3_grid` before PSMC namelist is read:

```
LvSMC   =  1
ISHFT   =  0
JEQT    =  0
NBISMIC =  0
CFLSM   =  0.7
DTIMS   =  360.0
RFMAXD  =  36.0
UNO3    = .FALSE.
```

```

AVERG = .TRUE.
SEAWND = .FALSE.
Arctic = .FALSE.

```

For the SMC6-25 grid its PSMC namelist has the following parameters:

```
&PSMC DTIMS=39600.0, LvSMC=3, JEQT=1344, Arctic=.TRUE. /
```

where DTIMS is the swell age (in unit of s) used to define the smoothing (diffusion) coefficient. RFMAXD is the maximum refraction angle in degree. It is recommended to be less than 60 degrees to avoid caustic-like focus of spectral energy. Setting it equal to one directional bin width will bring the refraction rotation scheme to be equivalent to the regular grid refraction term. The default value is set at 36 degree, which is used in the UKMO wave forecasting models. Users may change the default values by modify them in `ww3_grid.ftn` so that they do not need to be in the `ww3_grid.inp` PSMC namelist line, which has a built in length restriction of 80 characters in the present WW3 model. For the same reason, the default value for the 1-2-1 average is also selected as AVERG = .TRUE. because this additional smoothing is used in UKMO wave forecasting models.

The LvSMC integer represents the number of levels of the multi-resolution SMC grid. The above quoted line is for the SMC6-25 grid, which has 3 levels: the 6 km, 12 km, and the base level 25 km. The JEQT integer (1344) is a shifting number for conversion of the SMC grid cell y-indices to the regular grid j indices. It is equal to the distance from the regular grid y-origin to the SMC y-index origin (on the Equator for SMC6-25 grid and hence JEQT) and divided by the SMC size-1 unit length. Because the regular 25km grid y-indices starts from southern boundary of the model domain while the SMC6-25 cell y-indices are referred from the Equator, the SMC6-25 cell j indices have to be shifted by this number for mapping with the regular grid y-indices. There is a similar namelist integer parameter ISHFT for the x-index conversion to the regular grid i -indices. As the SMC6-25 cell x -indices share the same origin as the regular grid (at zero meridian) this parameter is not defined in the namelist but takes the default value 0. Also note that, the SMC6-25 cell indices are in units of the smallest cell (size-1) while the 25km regular grid is at the base level (size-4). So SMC6-25 cell indices are 4 times larger than the regular grid ones.

The following lines are added after the regular grid depth file line (which line is still kept to read the minimum depth parameter though the regular grid depth file is not actually read for a SMC grid):

```

32 1 1 '(....)' 'S6125MCels.dat'
33 1 1 '(....)' 'S6125ISide.dat'
34 1 1 '(....)' 'S6125JSide.dat'
31 1 1 '(....)' 'S6125Obstr.dat'

```

The regular grid sub-grid obstruction file read line has been moved after the cell and face array files because the smc cell only obstruction file requires the cell array for mapping the obstruction ratio.

If the model needs boundary conditions, users should set another PSMC namelist integer NBISM, which is the number of boundary cells. A non-zero NBISM number will invoke extra lines to read the boundary cell list from an extra input file and setup boundary condition interpolation arrays for the model. The boundary cell list file is specified in `ww3_grid.inp` by

```
35 1 1 '(....)' 'S6125Bundy.dat'
```

If NBISM is not defined in the PSMC namelist, it will take the default value 0 and tell the `ww3_grid` program to skip those lines as no boundary conditions are required. Note that SMC grid boundary conditions are set up by the boundary cell list (the sequential number of the boundary cells in the full cell array list) instead of using masks. To generate boundary conditions for other models, however, the SMC grid uses the normal longitude and latitude settings as a regular lat-lon grid model. This is also true for generating boundary conditions for a SMC grid model. Users need to convert the cell list into corresponding list of lat-lon pairs for the mother model to generate boundary condition files for it. The lat-lon pair list does not need to be in the same order as the boundary cell list. If no boundary

condition is required (`NBISMIC = 0`), the above line in `ww3_grid.inp` should be commented off with a first column `$` sign.

The old ARC switch used to include the Arctic part is removed from WW3 Vn7 and a new PSMC namelist variable, `Arctic`, is introduced to define whether the Arctic part is included. The `Arctic=.TRUE.` in the above PSMC namelist line tells `ww3_grid` that the Arctic part is included for the SMC6-25 grid and extra SMC grid input files are required for the Arctic part. The additional lines for Arctic cell and face arrays are specified in `ww3_grid.inp` by the following lines:

```
$ Extra cell and face arrays for Arctic part. JGLi16Jan2014
36 1 1 '(....)' 'SMC625BArc.dat'
37 1 1 '(....)' 'S625AISide.dat'
38 1 1 '(....)' 'S625AJSide.dat'
```

If the Arctic part is not required, these lines should be commented off as well. The input line for the regular grid masks file is kept though the masks file is not read for SMC grid. The masks are defined inside `ww3_grid` for the SMC grid model using the cell array (and boundary file if any).

```
39 1 1 '(....)' 'NAME' 'S625Masks.dat'
```

As SMC grid shares some grid variables with regular lat/lon grid, the grid parameters for a corresponding regular grid at the base resolution are provided in the same way as a regular grid, except for the grid type string which should be specified as ‘`SMCG`’ as shown below:

```
$ 'RECT' T 'NONE'
  'SMCG' T 'SMPL'
    1024    736
    0.35156250 0.23437500 1.
    0.17578125 -82.3828125 1.
$
```

Once these input files are put in place, the `mod_def.ww3` file is generated with the `ww3_grid` program as for the regular grid model. The SMC grid WW3 model can then be run the same way as a regular grid model, drive by wind forcing at the base resolution. See the WW3 manual for running the `ww3_grid` and the `ww3_shell` program.

A sea point wind option has been added since WW3 V6.07 and it could be activated by the PSMC namelist variable, `SEAWND = .TRUE.`, which will trigger the `ww3_shel` or `ww3_multi` program to read sea-point only wind input files. The sea-point wind input files are in the same format as the regular wind files except for that the wind array is in the shape of `(NSEA, 1)` instead of the regular grid shape of `(NX, NY)`. This sea-point wind option provides a possible way to mix different resolution winds to drive multi-resolution SMC grid wave model and it also reduces model run time as wind over land points are no longer processed.

Output from the SMC grid WW3 model can be saved as the regular base-level lat-lon grid ones or as sea-point only output. The former regular grid output will lose the refined resolutions. The sea point only format saves output at all the SMC cell points in the same order as the input cell array. From WW3 V5.16 onward, the `ww3_outf` program could be used to generate cell-only text output files by the type-4 option. Because the output cell sequence is the same as the SMC grid input cell array, there is no need to save mapping info in the output files and the re-mapping could be simply done with the input cell array for visualization. There are some example IDL and Python programs under the sub-directory `smc_docs/SMCG_TKs/` in the WW3 package to illustrate how the text output files could be mapped into a global view frame. The `ww3_ounf` program is also enabled to convert SMC grid output into either sea-point only or regularly gridded netCDF outputs.

5. SMC grid propagation test

There is a pure spectral propagation test for the SMC grid input files before they are used for the WW3 wave model. This spectral test can also be used for validation of other propagation features, such as the proposed map-east direction method in the Arctic and the rotation scheme for the wave refraction. An idealised wave propagation test on the SMC6-25 grid in an ice-free Arctic is used here for demonstration. The test includes all the 4 terms (advection, diffusion, refraction and GCT) in (1) but does not have any source term. The transient zone from the global to the Arctic parts is around 86°N and the map-east reference direction is used within the Arctic part (area within the red ring in Fig.1).

A constant wave spectrum is assigned to all cells within a 3.75° radius from the N Pole. The wave spectrum has 36 directions and a fixed frequency at 0.0625 Hz or period T = 16 s. Because all frequencies show the same directional pattern, one frequency is sufficient for this demonstration. The initial wave spectrum is defined by

$$E(\theta) = \begin{cases} E_0 \cos^2(\theta - \theta_p), & \text{for } |\theta - \theta_p| < \pi/2 \\ 0, & \text{Otherwise} \end{cases} \quad (14)$$

where $E_0 = 50/\pi$ is a constant, θ_p is the peak direction. The transported spectrum is integrated as the wave height, $H = \sqrt{\int E d\theta}$, like the SWH used in wave models apart from a constant factor. The gravity depth is about 64 m for the given frequency (0.0625 Hz) ocean surface wave and its group speed is about 12.5 m s⁻¹ in deep waters. The time step is 300 s for the smallest (6 km) cells and is increased to 600 and 1200 s for the 12 km and 25 km cells, respectively, resulting in a maximum Courant number of 0.929.

The initial wave height field is shown in the row (a) of Fig.4 and its non-zero wave height is constant 5 units. Note the wind-sea spectrum (14) has a peak direction θ_p from its reference direction. The peak direction is set to be 45° towards the northeast for the two round patches and the southern belt as indicated by the spectral roses in Fig.4. For the northern belt the peak direction is at -45° towards the southeast. Another round patch of the same size as the Arctic one is initialised in the Atlantic close to the Equator (centred at 33°W 5°N) to test the map-east method. Because the Arctic and global parts use different reference directions, the peak direction of the initial spectrum varies with longitude in the global part. Inside the Arctic part, however, the reference direction is fixed at the map-east so the initial spectral peak direction is constant for all non-zero cells there.

The middle row (b) of Fig.4 shows the idealised wave propagation result after 40 hrs. The initial waves have travelled about 1800 km and typical wave propagation features are revealed. The Arctic patch is almost out of the Arctic part and shows a similar distribution as the Atlantic patch. The northern belt in the Atlantic has passed the British Isles and reached the Canary Islands. The blocking effects of the Azores islands are clearly illustrated. The northern belt in the Pacific shows the cutting effect by the Aleutian Islands. The southern belt has reached the southern coast of Australia and revealed the blocking by New Zealand and other Pacific islands. The stretching effect around the gravity depth is visible in the Great Australia Bight where the wave height (in colour green) is lower than those on the deep side (yellow-orange) and near the coastlines (orange-red). This stretching effect is difficult to see in wave models because it is usually muffled up by wind sea and other propagation effects, such as dispersion and refraction.

The lower row (c) of Fig.4 shows the propagation results after 80 hrs. By then the northern belt has cut through the Hawaii Islands, revealing their detailed blocking effects by the 8 main islands. The G25 and SMC25 grids can only resolve 4 islands out of the Hawaii archipelago. The southern belt is now abreast with the northern coast of Australia, pulling through the oceanic islands. The highest 6 km resolution in this SMC6-25 grid is, however, still not enough to show the atolls or coral reefs in the French Polynesian islands as demonstrated by Chawla and Tolman (2008) in a high resolution regional model and sub-grid

obstruction is required to represent the fine structure. Also note in row (c) of Fig.4, the slow GCT and GSE smoothing effects manifest themselves with the smoothly spreading of wave energy in the Southern Ocean and quickly filling up the shadows behind the wave-blocking islands. Smoothed wave propagation indicates that the input files for the SMC grid are set properly and are ready to be used for the wave model.

Because the polar region of the Arctic Ocean is still covered by sea ice, it is not practical to validate the map-east method against wave observations. Here a simple approach is used to assess the map-east method by comparing the propagation of the Arctic and Atlantic patches. If the two patches have similar propagation pattern, the map-east method may be deemed equivalent to the local east method. The two round patches are drawn side-by-side in Fig.5 for this comparison. The global perspective of the two initial round patches are shown in row (a) of Fig.4 and the non-zero wave height is constant 5 units. Because of the different shapes of the grid cells at the two sites, the Arctic patch has a round edge while the Atlantic patch has a stepped edge. Nevertheless, the two patches cover approximately the same area.

The two co-centred rings in the Arctic plots mark the transient zone from the local east to the map-east reference directions. The initial spectral peak direction θ_p is 45° from their reference direction, respectively, as indicated by the spectral roses in Fig.5. Because the Arctic part uses a fixed map-east reference direction, the initial spectral peak direction is constant within the Arctic part. In the global part, however, the local east reference direction changes with longitude and so the peak direction of the initial spectrum. Therefore the Atlantic round patch is initialised near the Equator to minimise the local direction change.

The middle row (b) of Fig.5 shows the two patches after 15 hrs of propagation. The centre of the Arctic patch has covered the transient zone. It is evident that there is no visible interruption of the patch distribution in the two reference direction parts. The Arctic patch is quite like the Atlantic one shown on the right side except for the fine cuttings caused by local islands. The bottom row (c) of Fig.5 shows the two patches after 30 hrs when the Arctic patch is out of the map-east zone. The two patches still share a quite close distribution in the deep waters. The blocking effects by local islands and water depth induced refraction and speed changes have left their unique marks on the two patches. These results confirm that the map-east method is effective for wave spectral propagation in the polar region and solved the polar problem in finite difference schemes on reduced grids. The transition between the two reference direction zones is smooth and does not cause any visible interruptions in surface wave spectral propagation.

This spectral propagation test model is initially designed for checking whether the SMC grid cell and face arrays are generated properly before they are used in the WW3 model. It is designed to run on desktop machines and has not been parallelised. A new parallelised SMC grid propagation model is now available. The parallelised model follows the same memory arrangement in WW3 for multi-node super computers. It uses the same SMC grid module in WW3 and some WW3 parallel subroutines as well for parallelisation. It can run in hybrid (MPI-OpenMP) mode on over a hundred computer nodes and is much faster than the original desktop program. This parallelised propagation model is used for SMC grid scalability and new parallel schemes studies. It is available on request now and will be made open access either with future WW3 public release or on a dedicated SMC grid toolkit web site.

6. Applications of SMC grids in the UK Met Office

The UK Met Office wave forecasting models have been using the SMC grid since 2016 and here list the main waver forecasting models and its configurations.

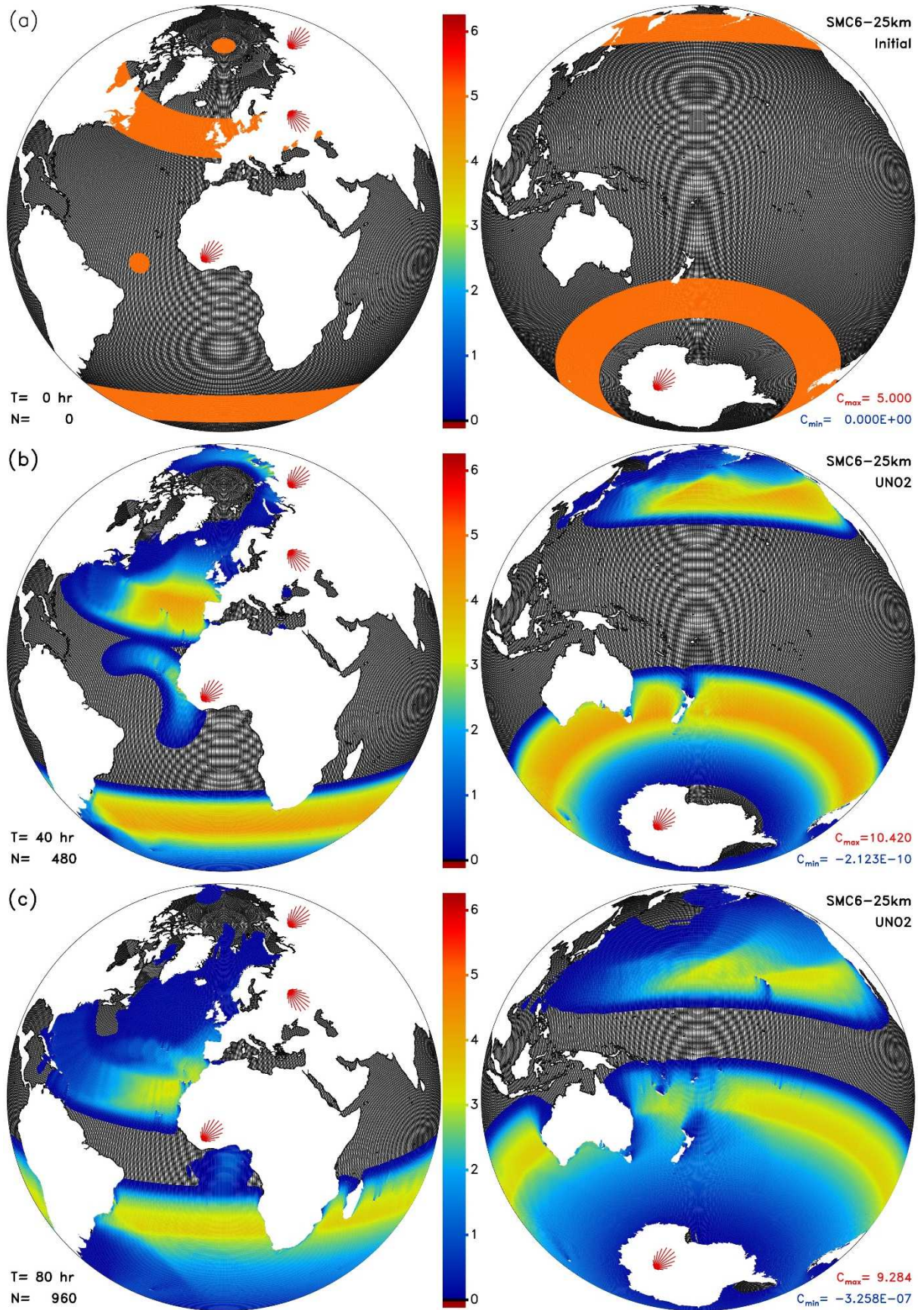


Fig.4. Idealised spectral wave energy propagation on a global SMC6-25 km grid.

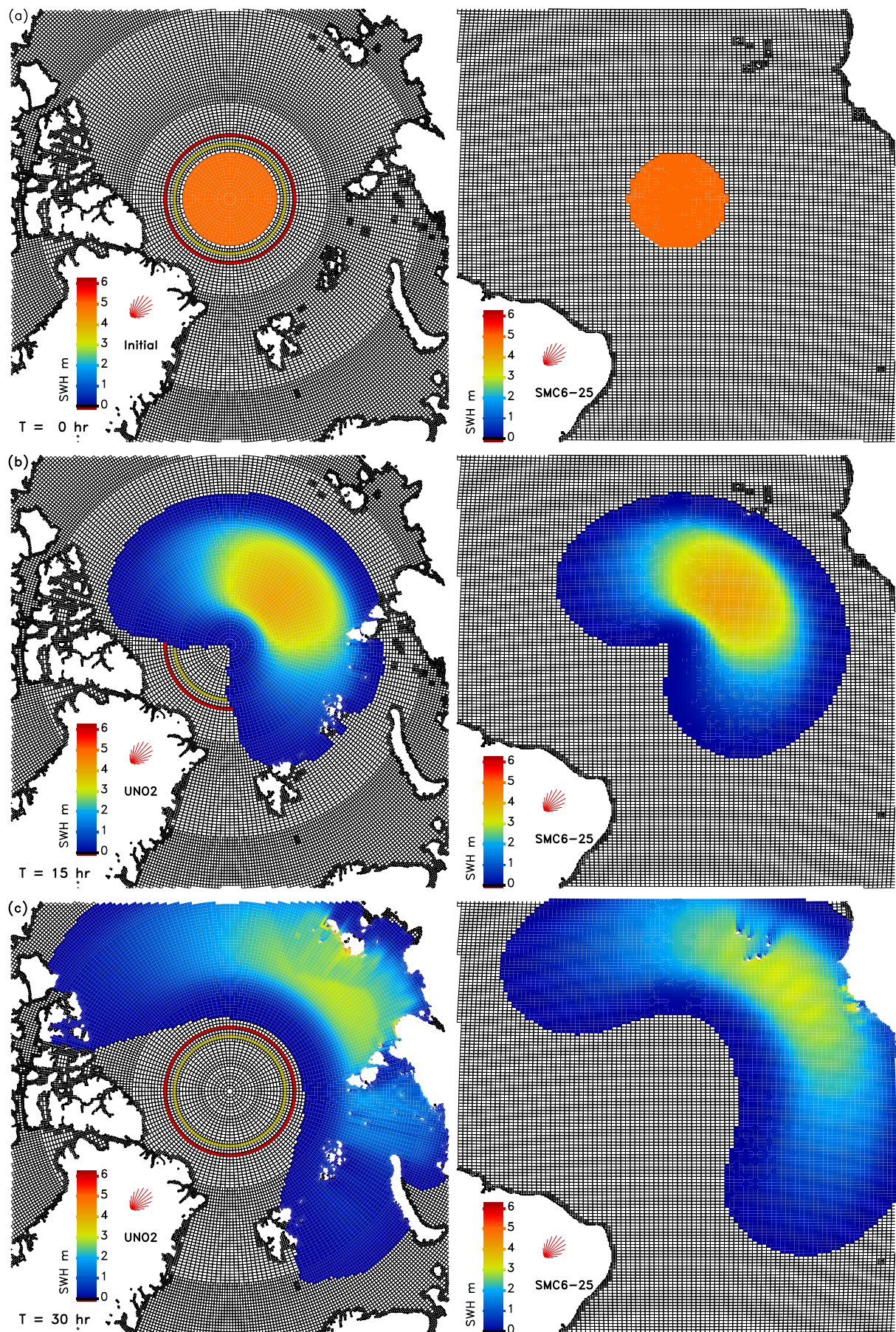


Fig.5. Comparison of the wave spectral propagation using Arctic map-east (left column) and the conventional local east (right column reference direction methods.

6.1 Global 3-6-12-25 km wave forecasting model

Since October 2016 the Met Office has updated its global wave forecast model to a 3-6-12-25 km 4 level SMC grid (SMC36125), replacing the old 35 km global multi-grid model (G35). The new global model has a base resolution of about 25 km in open oceans and refined to 12 and 6 km close to most coastlines (Li and Saulter 2014). Fig.6 zooms in the Arctic and European region of the SMC36125 global model and it has a refined area in the European waters at 12 km resolution and down to 6 and 3 km near coastlines. This refined area is intended to replace our European 8 km nested model. The total number of sea points in the SMC36125 grid reaches 592,570, more than doubled of the G35 sea points (~ 290,000). Spectral resolution is also increased from 24x25 in G35 to 30x36, or 80% increase, plus source terms update from ST3 to ST4, which alone costs 10% more in computing. Total increase of computing load is about 2 times of that of the G35 model.

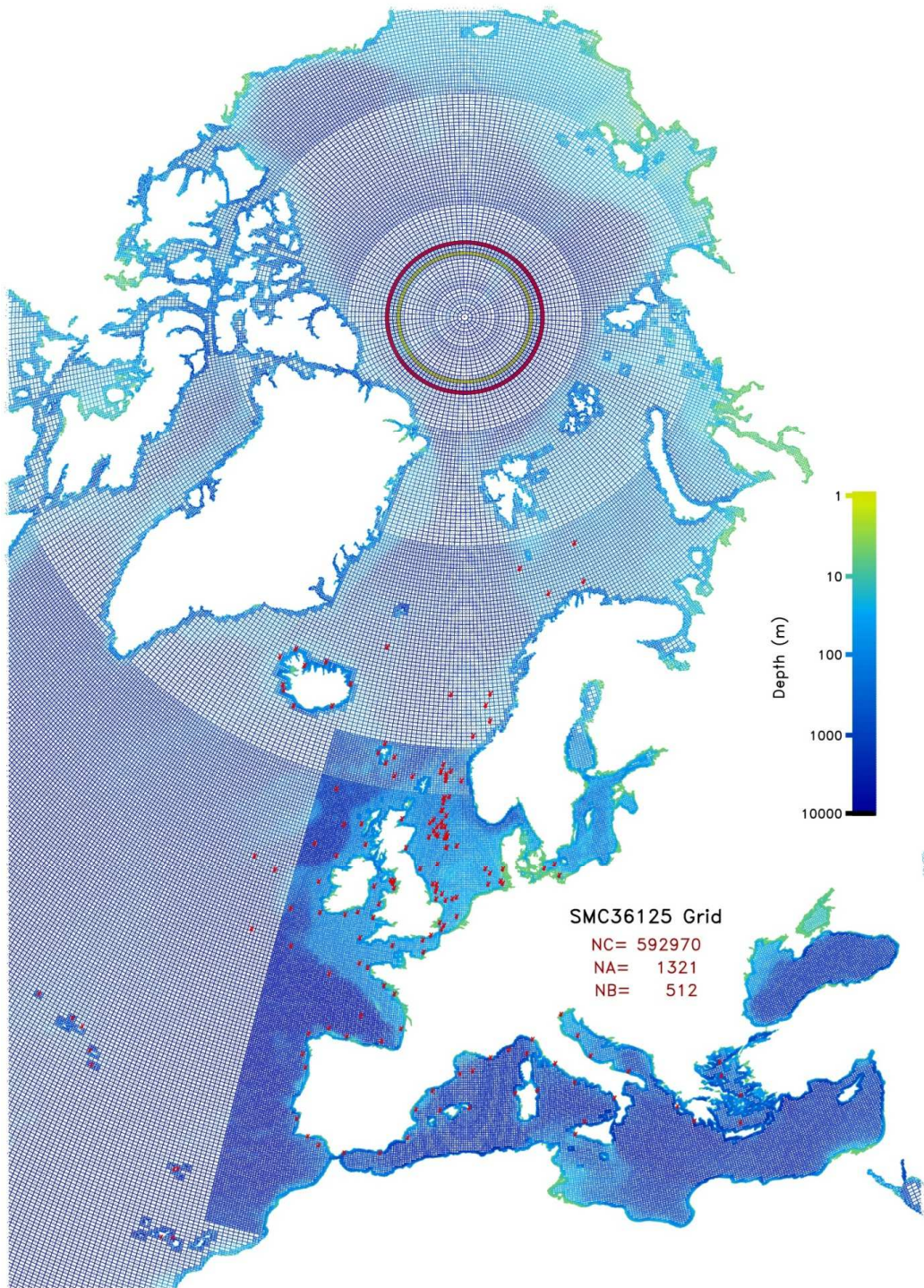


Fig.6. The Arctic and European region of the Met Office global 3-6-12-25 km SMC grid.

The model performance is significantly improved after this update as indicated by the JCOMM buoy data inter-comparison (Bidlot et al 2007). Fig.7 shows the scatter indicator (SI) plots before and after our global model update, in comparison with other global wave forecasting models. The Met Office forecast (MOF) model is indicated by the green line in Fig.7 and the October 2016 plot (top panel in Fig.7) used our old global wave model data while the November 2016 plot (lower panel in Fig.7) were draw with our updated SMC36125 model data. The improvement is significant considering the slight increase in computational cost.

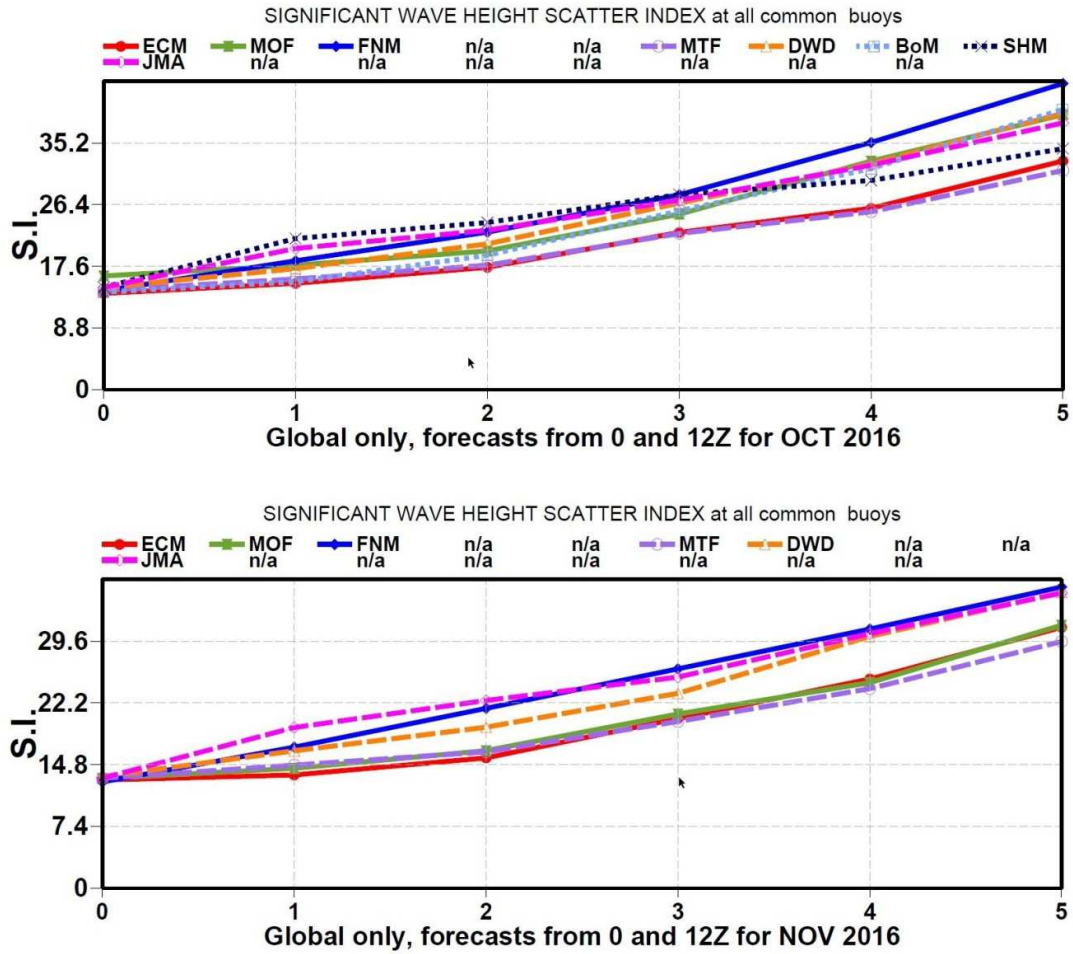


Fig.7. Scatter indicator plots of the ECMWF inter-comparison of 5-day wave model forecasts against all available buoy data for October and November 2016. The Met Office model performance is indicated by the forest green line (MOF).

6.2. North Atlantic ensemble model

The second SMC grid wave model used in the Met Office wave forecasting system is the north Atlantic wave ensemble model, which uses a grid similar to SMC36125 but removes the European refined area and all ocean surface except for the north Atlantic main water body (see Fig.8). To minimise boundary input, the selected north Atlantic domain follows coastlines all the way except for a few short crossings, such as the over the Gibraltar Strait, Baltic Sea, Hudson Bay, and particularly over the Southern Atlantic Ocean along the Tropic of Capricorn. To minimise the computing cost, the base resolution 25 km cells are used as much as possible and the highest resolution 3 km cells are used only near European coastlines. A deterministic 2D wave spectral boundary condition is provided by our SMC36125 global model, only for the southern crossing along the Tropic of Capricorn. The ensemble model is driven by a set of 18-member perturbed wind forcing and run 4x18 times a day to provide ensemble forecasts for UK coastal areas.

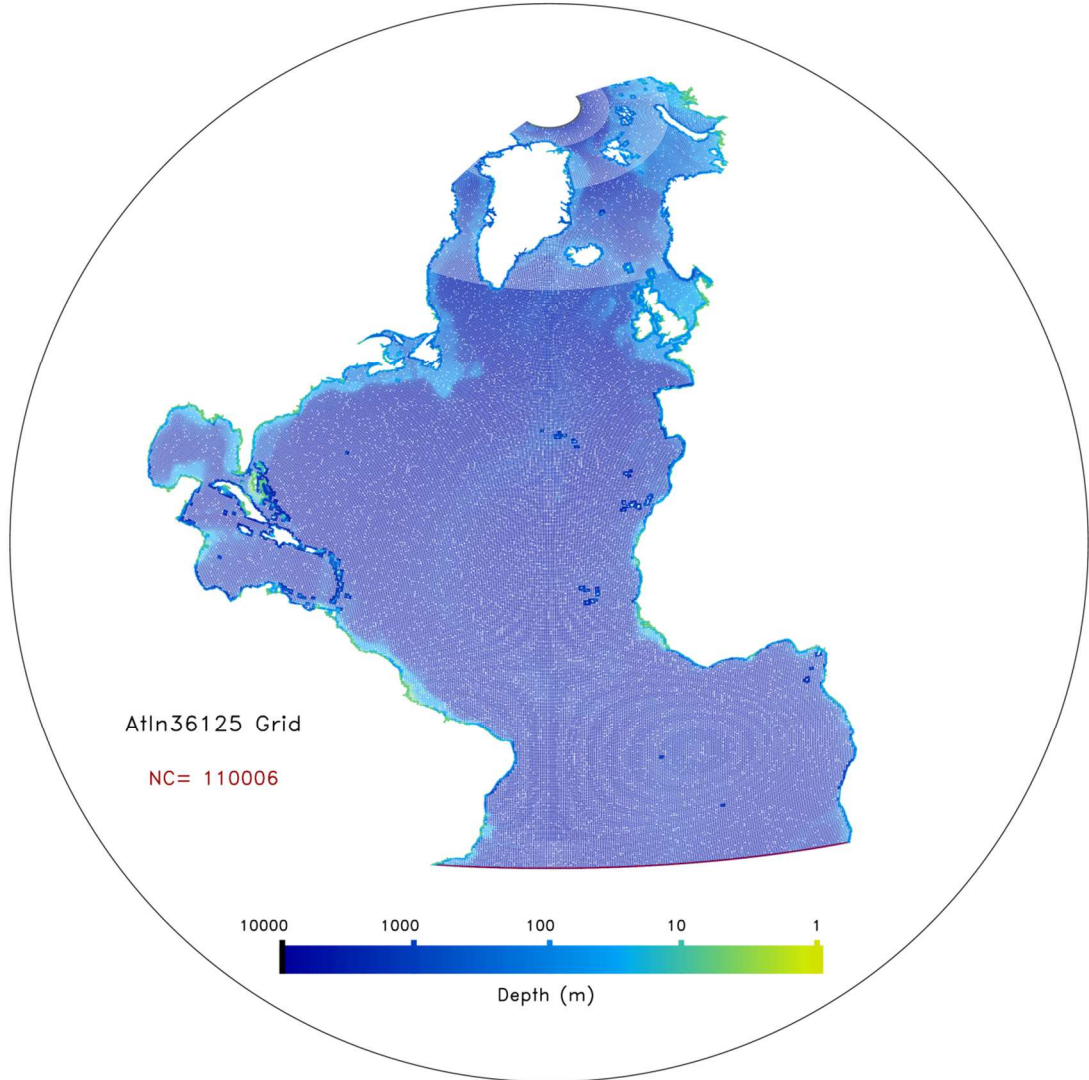
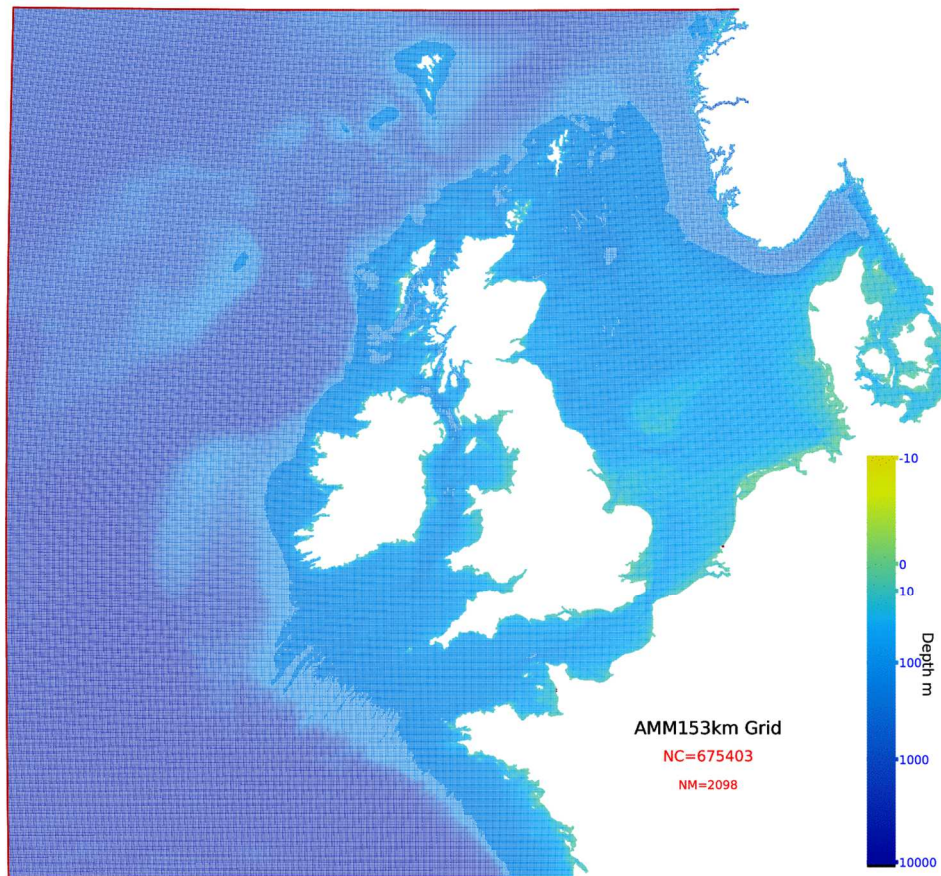


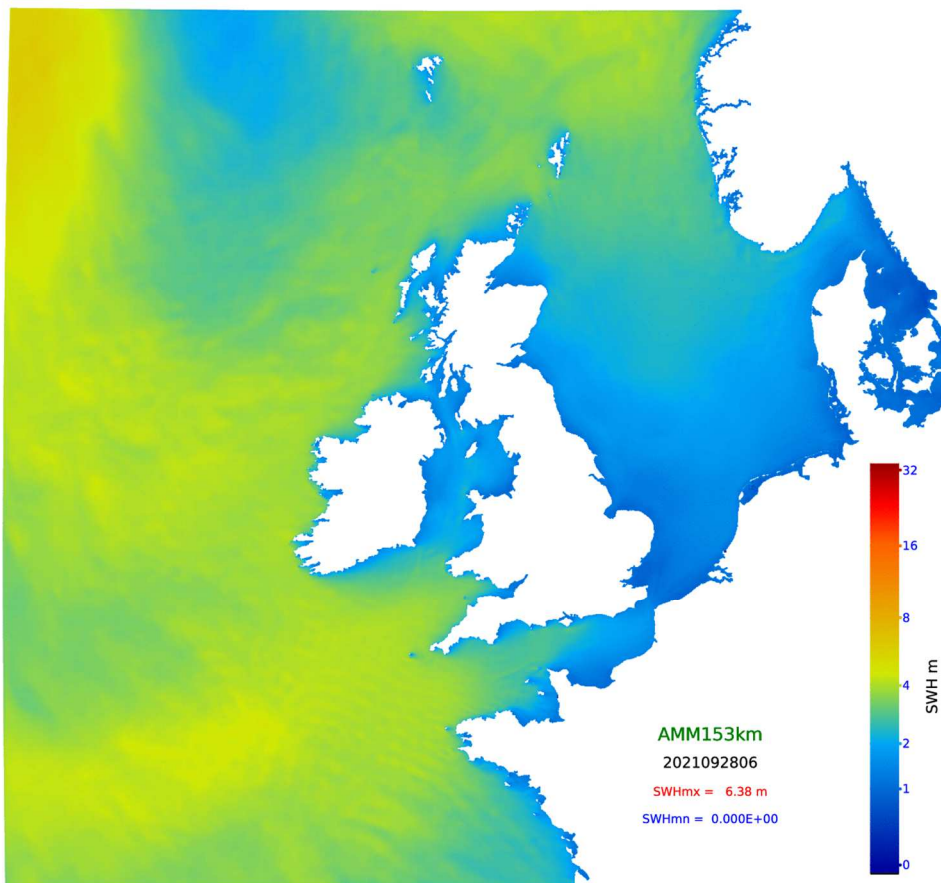
Fig. 8. The Atlantic SMC36125 grid ensemble model.

6.3 UK 1.5-3 km rotated SMC grid model

The UK 1.5-3km SMC grid model uses a rotated grid (rotated north pole at 177.50°E 37.50°N) with a uniform increment of 0.0135° in each dimension for the 1.5 km refined cells and a base resolution of 0.0270° , or about 3 km, for the rest (see Fig.9a). The refinement criterion is based on both proximity to the coast and water depth. The 1.5 km cells are used for all locations where averaged depths are less than 40 m. The grid covers a region from approximately 45°N , 20°W to 63°N , 12°E and is derived from a 1.5 km ocean model, which generates the input surface current for the wave model. This model has replaced the old UK 4 km regional model since 2019. Validation work has been done and the model performs well except for a small but stubborn problem with the current induced refraction. Somehow, the current gradient induced wave-number shift may trigger an unknown mechanism in the non-linear wave interaction terms (both DIA or WRT options), which generate extra wave energy and lead to spurious high waves around the French island (Isle of Ushant). This is mitigated by switching off, or massively limiting, k-shift effects. The MLIM option for a limiter of shallow water and steepness may also reduce the erroneous high waves. This UK 1.5-3 km SMC grid wave model is also used in the Met Office regional coupled system for wave climate studies. In 2024, the model is updated with wet/dry option for coupled system and cell wet/dry status is updated with combined water depth from ocean model sea-level input. The black cells in Fig.9b indicate the dry cells. This allows coastal flooding to be simulated in coupled climate system.



(a)



(b)

Fig.9. The rotated SMC 1.5-3 km UK grid (a) and its SWH output from WW3 model (b).

6.4 Global SMC 50 km grid wave model for coupled system

A 50 km SMC grid global wave model including the whole Arctic is used for wave climate studies in the Met Office coupled system (including atmospheric, ocean, ice, and wave models). The relaxed CFL restriction and full Arctic inclusion in the SMC50km grid allow an efficient wave component in the coupled system to study various climate scenarios, including the fully opened ice-free Arctic case. This SMC50km grid is used as a sample grid in the WW3 model public release and users may try to generate it from files provided in the WW3 V6.07 model package, particular in `smc_docs/SMC_TKs/`. A 4-level 6-12-25-50 km grid (SMC61250) has been tested and is proposed to replace the single resolution SMC50km grid for coupled systems. It only increases the computing load by a fraction but improve the wave prediction dramatically because of the improved blocking effects by resolved small islands at the 6 km resolution. A brief description of the SMC61250 grid may be found in a recent paper (Li 2019).

The following steps may be used to generate the SMC50km grid and run the wave model WW3 V5.16, plus some sample visualization.

- 1) To generate SMC50km cell arrays, run IDL program `Glob50SMCeles.pro`, which will read the bathymetry data `G50kmBathy.dat` and produce the global cell array file, `G50SMCelesA.dat`, including the Arctic.
- 2) Decide how large the Arctic part you like and divide the `G50SMCelesA.dat` into the global and Arctic parts. We chose all cells above $\sim 84^{\circ}\text{N}$ or $j \geq 179$. Note that there are 4-overlapping rows between the global and Arctic part, so the global part actually contains all cells up to $j = 182$.
- 3) Sort the global part cells with Linux script `countcells`. The Arctic part is already in the right order so there is no need to sort it but the first count line has to be entered manually by counting the total number of cells in the Arctic part and the boundary cells for the first two and next two overlapping rows. In our example file `G50SMCBAr.dat` the first count line is
 489 128 128
 You may now visualize the SMC50km cells with the IDL program `g50smcgrids.pro`, which has some tuneable parameters to choose your viewpoint and area. The projection will be saved in 3 data files, which can be used later for wave output visualization from the same viewpoint as the grid.
- 4) Generate face arrays with `G50SG1Side.f90` and `G50SACSide.f90` for the global and Arctic part, respectively. They will read the sorted cell arrays as input.
- 5) Sort the face arrays (output from `G50SG1Side.f90` and `G50SACSide.f90`) with the Linux script `countijsd`.
- 6) Generate the subgrid obstruction ratio with `Glob50SMCObstr.pro`, which will read the subgrid obstruction data (on full grid), `G50kmObstr.dat`, and produce a SMC cell only sub-grid obstruction file `G50GOBstr.dat`, plus a text information file for setting up the regular grid input files (wind, ice, etc if any).
- 7) Prepare the model input files. Here are the list of files in `inp/`

```

23932 Nov 18 2013 G50AISide.dat
29276 Nov 18 2013 G50AJSide.dat
5356170 Oct 20 2014 G50GISide.dat
5792134 Oct 20 2014 G50GJSide.dat
537907 Oct 20 2014 G50GOBstr.dat
13223 Oct 20 2014 G50SMCBAr.dat
2904635 Oct 20 2014 G50SMCeles.dat

```

```

26530 Apr 13 15:50 ww3_grid.inp
3146 Apr 5 10:55 ww3_outf.inp.template
7097 Oct 4 2013 ww3_outp.inp.template
8770 Apr 5 13:50 ww3_shel.inp.template
3401 Dec 20 2012 ww3 strt.inp

```

Note the *.inp.template files require substituting the model start/end times to generate the final *.inp files.

8) Prepare the forcing wind, ice and current files if any. These forcing files remain the same as on a regular lat-lon grid. The corresponding regular grid settings are available from the inp/ww3_grid.inp.

9) Compile the WW3 model with the given switch file switch for series executables or for parallel ones by swapping 'SHRD' with 'DIST MPI' in the switch file.

10) Run the ww3_grid program to generate the inp/mod_def.ww3 file

11) Run the ww3_shel with all input files to generate wave model output.

12) Post-processing from out_grd.ww3, depending on which format you like. We use the full text output converted by ww3_outf (type 4) and then visualized with the idl program smc_docs/SMCG_TKs/g50smcwhglb.pro, which will use the same projection as saved in step (3b) for the SMC50km grid visualization.

7. Applications of SMC grid around the world

7.1 The Great Lakes SMC0512 grid

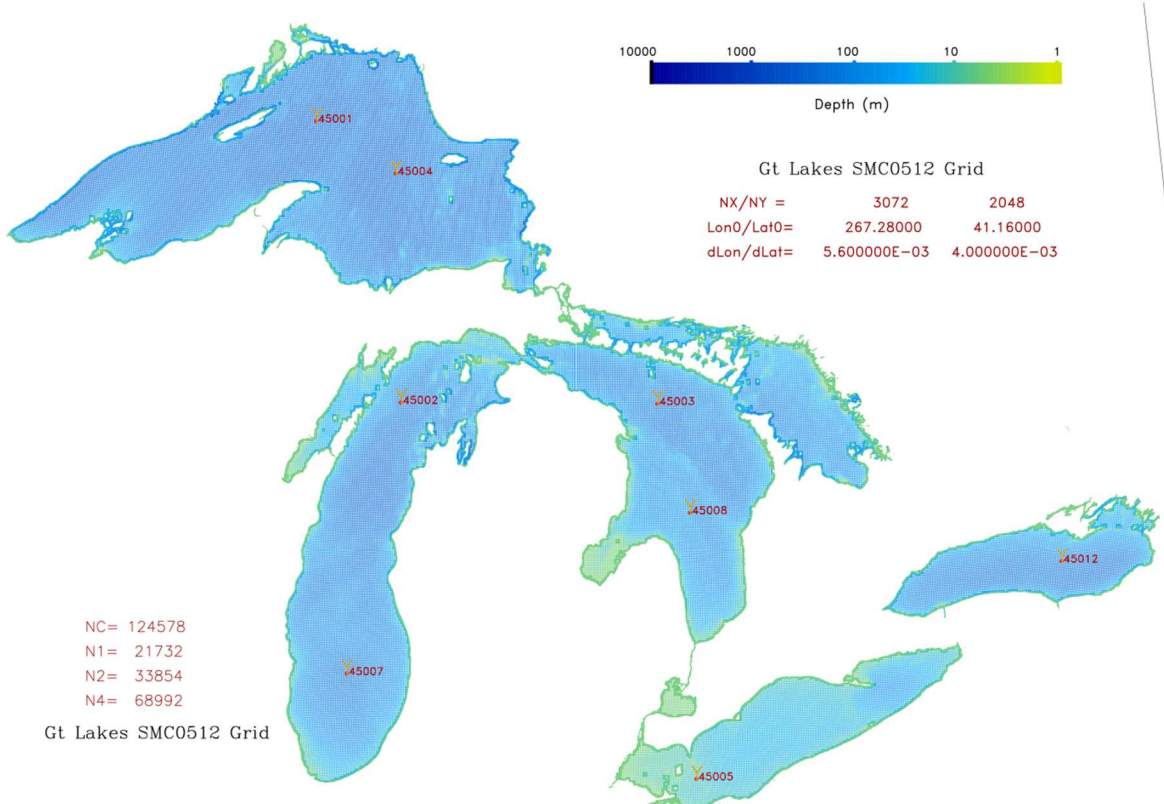


Fig.10. The SMC 0.5 – 1 – 2 km grid for the Great Lakes.

This is a regional model to cover the Great Lakes at variable resolution from 0.5 km to 2 km (Fig.10). As the Great Lakes are isolated from the oceans, this model domain does not need any boundary conditions. Also note the SW corner of the corresponding regular grid at 2 km resolution is chosen as the SMC grid index reference point so the index shifting numbers for the SMC0512 grid becomes zero. The model is designed for a research project in NCEP/NOAA to compare the different grids in the WW3 model, including the regular lat-lon grid, the curvilinear grid, the triangle cell unstructured grid, and the SMC grid. The project is stranded for some reasons and has not finished yet.

7.2. The Arctic wave climate system

This is an application in Environment Canada for wave climate study over the Arctic (Casas-Prat and Wang 2020). It consists of an Arctic regional model at 12-25 km resolution and a global 50-100 km SMC grid to generate boundary conditions for the Arctic regional model. Only the regional Arctic model 12-25 km SMC grid is shown here in Fig.11.

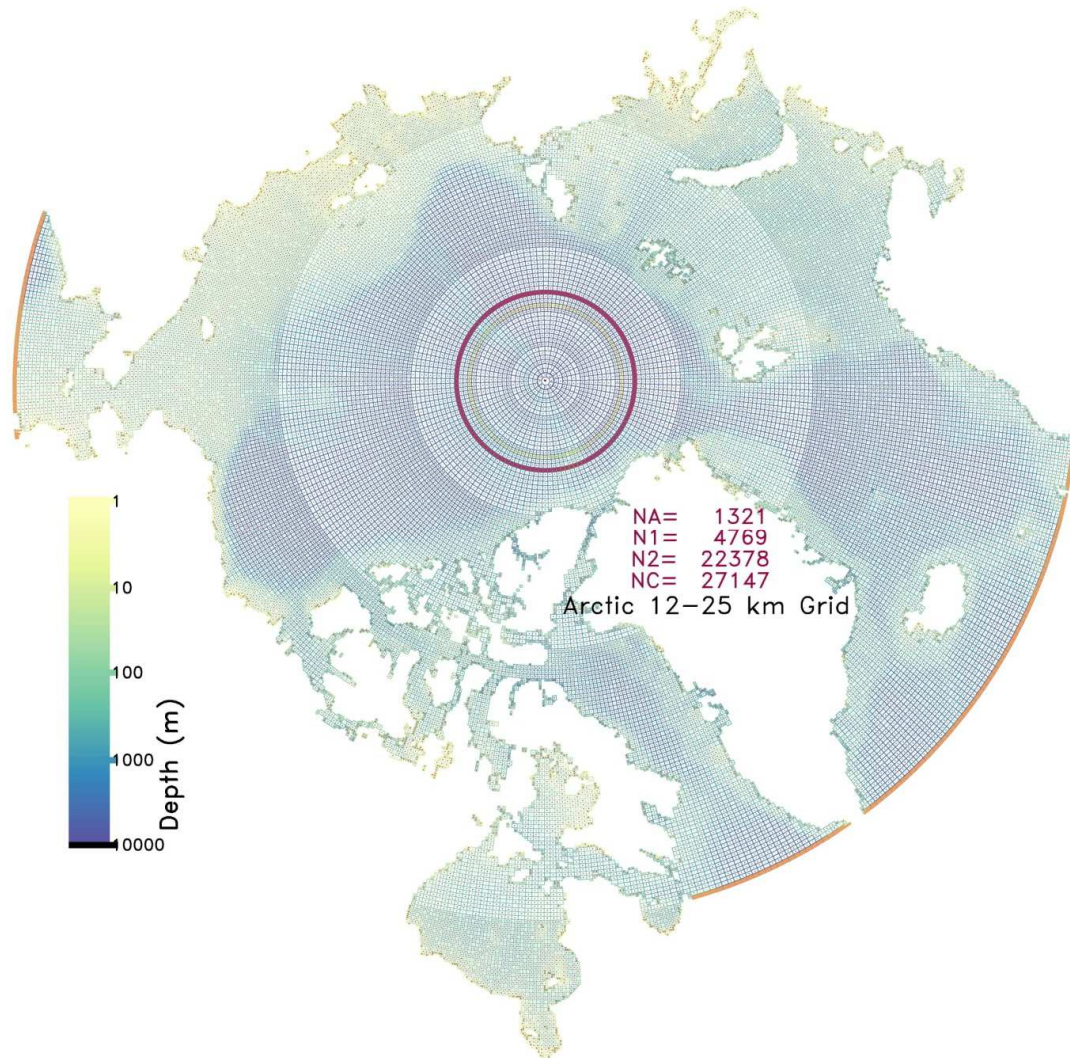


Fig.11. The EC Arctic wave climate model. Courtesy of Dr Mercè Casas-Prat (EC).

7.3 The SMC36125 Mediterranean model

This is a regional cut out from our SMC36125 north Atlantic ensemble model grid, covering the Mediterranean Sea only (see Fig.12). Boundary conditions for the short crossing at the Gibraltar Strait can be ignored if the area of interest is away from it. Two European partners, the Spanish UPC and the Italia CNR-ISMAR, have shown an interest in using this model for their regional wave environmental studies.

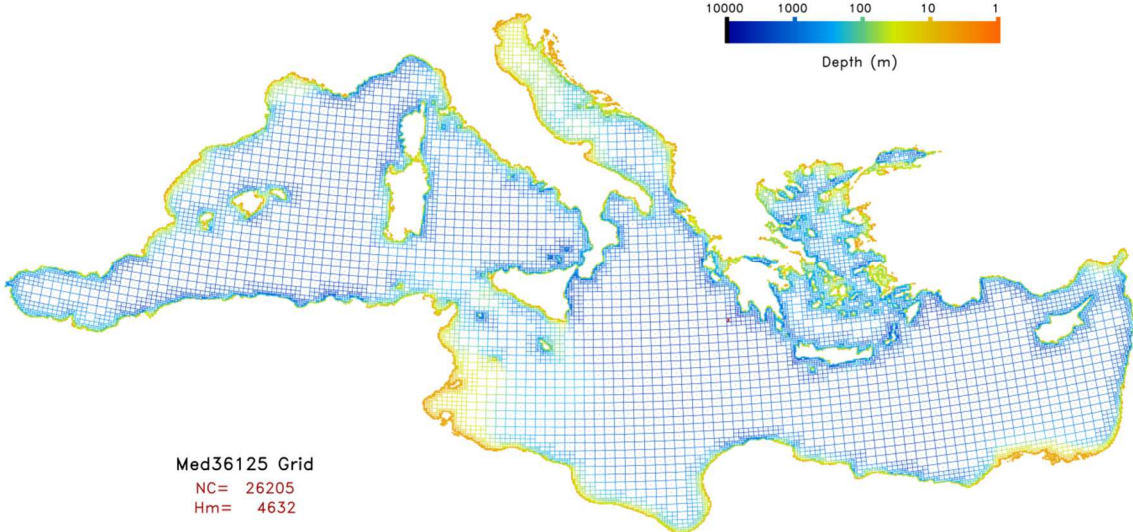


Fig.12. The SMC36125 Mediterranean grid.

7.4. The Gulf and Mexico and Caribbean Sea 12-25 km model

This Gulf of Mexico and Caribbean Sea 12-25 km SMC grid (see Fig.13) wave model was created for an Australian project to study hurricane wind effects on wave generation. Unfortunately, the model was abandoned at the last minute due to a current induced refraction problem in the WW3 V4.18 SMC grid module. This problem has since been found to be a mixture of a code bug and interactions between the current gradient induced wave number shift and the non-linear wave interaction schemes (both DIA and WRT). A temporary remedy to this problem is either to suspend the current gradient part in the wave number shift term or switch off the wave number shift term completely. It will not cause any noticeable change in the wave output fields except for removing those spurious high waves at strong current gradient area.

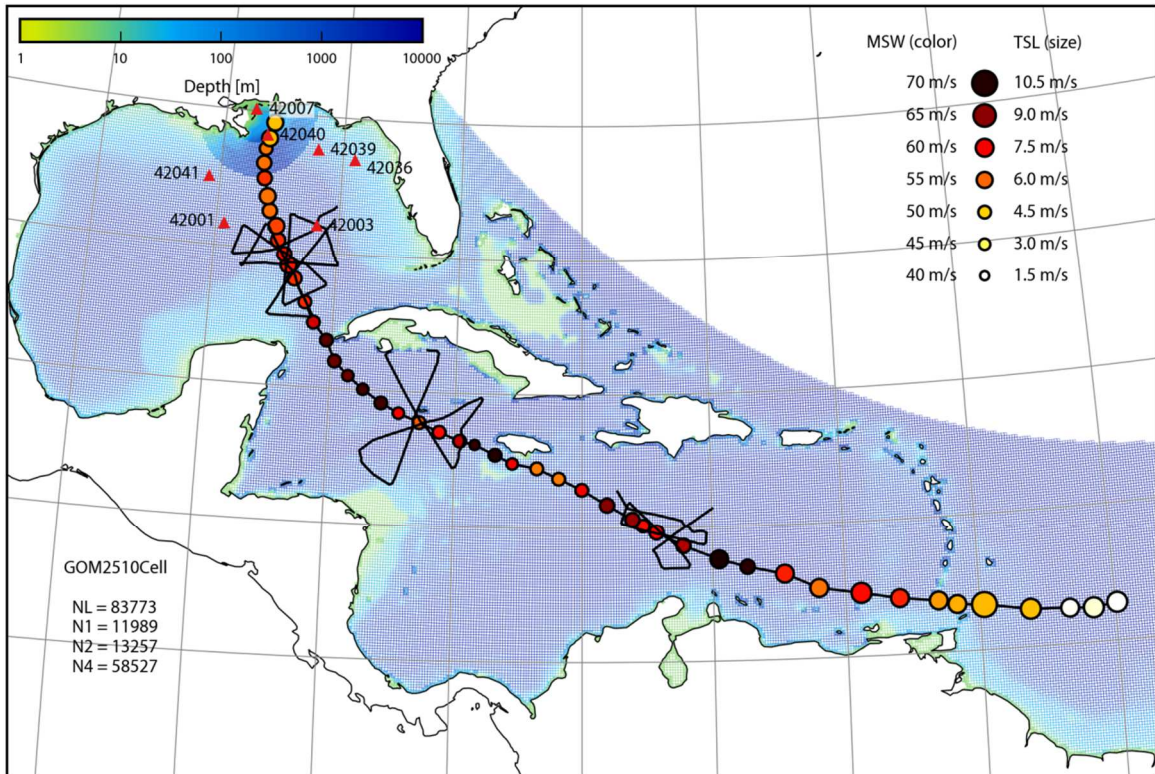


Fig.13. The Gulf of Mexico and Caribbean Sea 12-25 km SMC grid. Courtesy of Dr Qingxiang Liu (UM, Australia).

7.5. The rotated SMC grid Arctic model

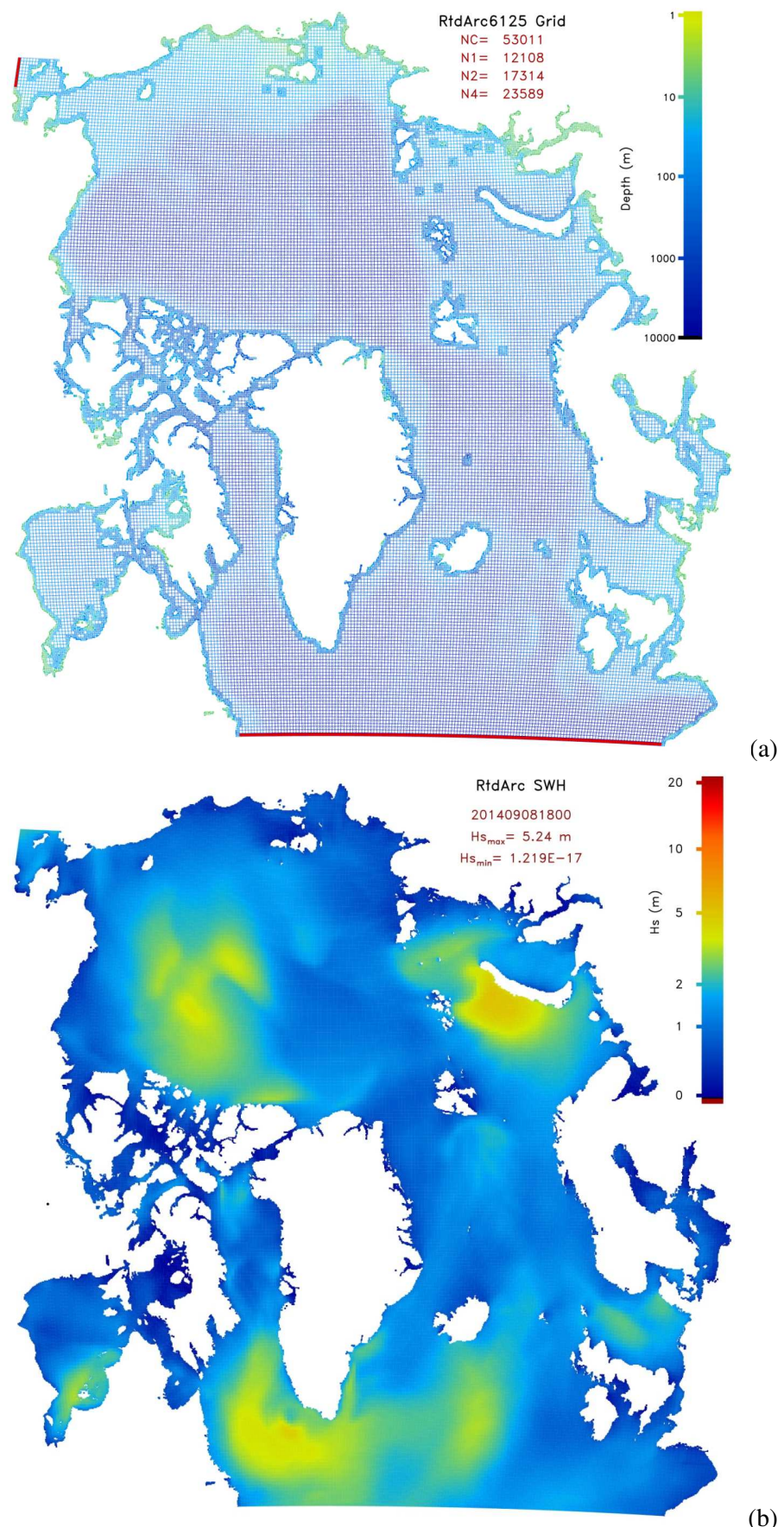


Fig. 14. The rotated SMC grid Arctic model at 6-12-25 km resolution (a) and its SWH field (b).

This model is proposed to replace the Environment Canada Arctic regional model. It uses a rotated SMC grid (the rotated north pole at 135°E and 10°N) with uniform size-1 increment at $\text{dlon} = \text{dlat} = 0.0625^\circ$ and 3 resolution levels at about 6-12-25 km (Fig.14a). One advantage to use a rotate grid is that there is no need for the map-east system in the high latitude region as it has changed Arctic into an equivalent Equatorial area. Another advantage of the rotated grid is the evenly spaced mesh within the model domain. The model has been compared with our operational global SMC36125 model and they agree well. A sample SWH output in an ice-free case from this rotated SMC grid Arctic model is shown in Fig.15. The model was driven by our global 17 km wind and 2D spectral boundary conditions for the red cells in Fig.14 are provided by our SMC36125 global wave model. Note that the forcing wind has to be converted into the rotated grid orientation before feeding into the model. The 2D spectral boundary conditions are, however, kept in the standard lat-lon grid orientation for the convenience of generation them by standard lat-lon model. The boundary 2D spectra will be converted to the rotated grid orientation inside the WW3 model.

7.6. The west Pacific regional wave forecasting model

The National Marine Environment Forecast Centre (NMEFC) of China replaced their west Pacific nested wave forecast system with a 6-level SMC grid model in 2020 (Hou et al 2022). It is more efficient than their old nested models and simplified their forecasting and postprocessing. Their improved SMC grid generating program is available on request. A group from the Ocean University of China (OUC) also used the SMC grid wave model for their studies of Arctic wave climate and Stoke drift effect (Li et al. 2021).

7.7. The Australia Bureau of Meteorology global forecast model - AUSWAVE-G3

A new wave forecast system was developed in the Australia Bureau of Meteorology to replace its old global and national wave forecast models. The new wave model (AUSWAVE-G3) uses the SMC grid at 12km base spatial resolution globally with refinement around sub-grid scale features at ~6km resolution (Zieger and Greenslade 2021).

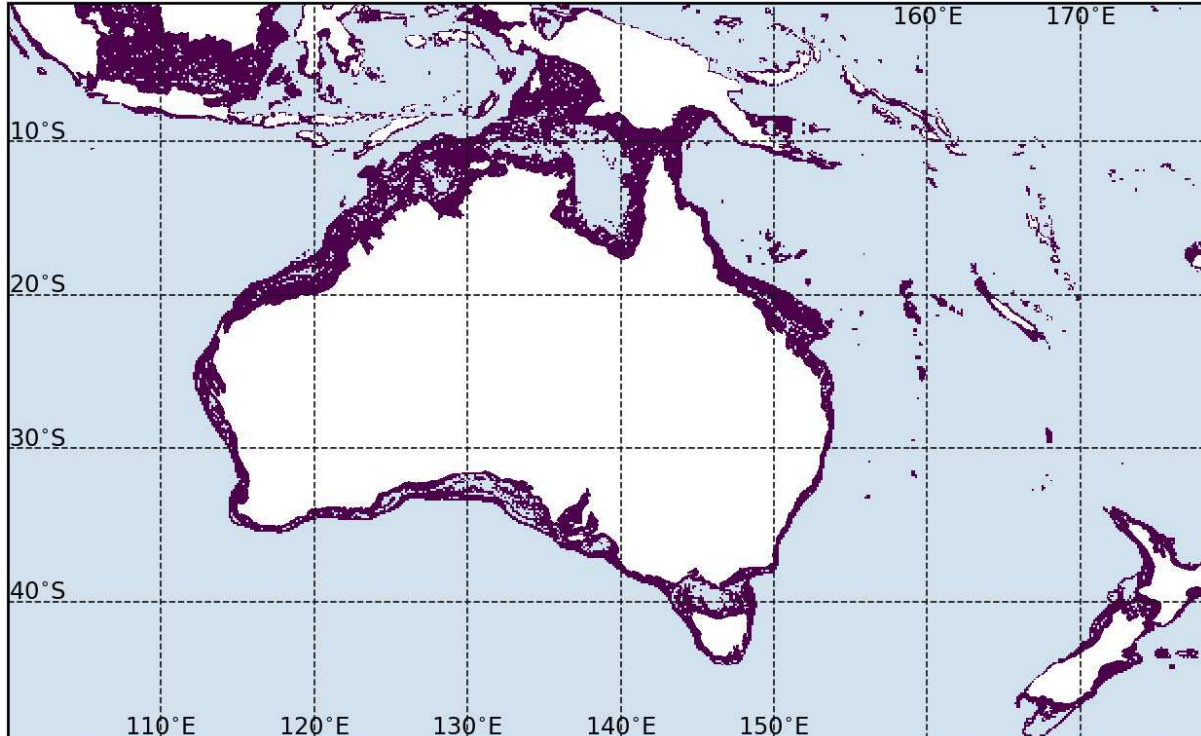


Fig.15. The BoM global SMC wave forecasting model grid around Australia area. Shading shows grid resolutions at $1/8^\circ$ (pale blue) and $1/16^\circ$ (purple). Courtesy of Dr Stefan Zieger (BoM).

7.8. East Russia and Arctic forecasting model

Dr. Alexander Vrazhkin has set up SMC grid wave forecasting models for East Russia (Sea of Okhotsk) and the Arctic regions in Hydrometeorological Institute (Vladivostok, Russia) at two

resolution levels ($4' - 8'$). Three-level SMC grids at $4'-8'-16'$ spatial resolutions are also tested but they are inferior to the 2-level ones, possibly due to the reduced wind forcing at $16'$ spatial resolution.

8. Summary and conclusions

The SMC grid is briefly reviewed and existing applications of this grid inside and outside the UK Met Office are summarised. This unstructured, multi-resolution latitude-longitude grid, which incorporates a practical solution to the polar problems, has shown its efficiency and convenience in various operational and research wave models. The Met Office global wave model update in October 2016 to a 3-6-12-25 km SMC grid is a successful demonstration of how the grid could help improve model performance without majorly increasing computation demands. The SMC grid supports flexible domain shapes and refined resolution in desired areas, making it suitable for both global and regional models. It retains the quadrilateral cells as in the standard lat-lon grid so that the efficient finite difference schemes could be used. Sub-timesteps are applied on different cell sizes to speed up propagation calculations, with a choice of 2nd or 3rd order advection schemes. Grid cells are merged at high latitudes to relax the CFL restriction and a fixed reference direction is used to define wave spectra in the polar region so that the SMC grid can be extended to the full globe, including the Arctic. The multi-resolution refinement is particularly useful to resolve small islands and coastline details, which are important in ocean surface wave propagation but could be too expensive in standard lat-lon grid models. The SMC grid package in WW3 has been improved to expand the usage of modern supercomputer resources by hybrid parallelization and a newly introduced multi-grid option. A sea-point wind forcing option opens the door for mixing different resolution winds to drive a multi-resolution model and it also reduces model run time because the spatial interpolation for the wind field is done prior to the model run.

The SMC grid has been implemented in the WAVEWATCH III community wave model since V4.18 and updated in the subsequent versions (V5.16, V6.07 and the coming V7.xx) with some bug-fixing and added new features. This grid has caught the attention of a few international users and collaborators, thanks to the widespread user network of the WAVEWATCH III model. Four operational and research SMC grid models have been used in the Met Office now, including the global SMC36125 operational wave forecast wave model, the north Atlantic ensemble model, the global 50 km SMC grid wave model in coupled climate system and the rotated SMC grid UK 1.5-3 km regional model. Outside the Met Office, a few SMC grid regional and global models have been used or in preparation. They are the Great Lakes 0.5-1-2 km SMC grid model for a NCEP/NOAA research project, the Environment Canada Arctic climate system (consisting of the 12-25 km Arctic SMC grid model and the 50-100 km global SMC grid to generate boundary conditions), the Gulf of Mexico and Caribbean Sea 4-8-16 km SMC grid model for hurricane studies in an Australia project, the Mediterranean Sea SMC36125 grid model for our European partners (UPC, Spain and CNR-ISMAR, Italia), and west Pacific multi-resolution regional SMC grid wave forecasting model in NMEFC, China, the AUSWAVE-G3 global 2-level (6-12 km) SMC grid forecasting model, and the Russian regional SMC grid wave forecasting models for the Sea of Okhotsk and east Arctic. The combination of rotated lat-lon grid and the SMC grid has created a more suitable platform for high latitude regional models than the SMC grid on the standard lat-lon grid. A rotated SMC grid Arctic model has been demonstrated to show its evenly spaced mesh in the whole Arctic region and the minimal changes required to run the model. It is expected that more users will find applications of this grid in their wave forecasting and marine environmental studies.

References

- Booij, N., L.H. Holthuijsen, Propagation of ocean waves in discrete spectral wave models, *J. Comput. Phys.* **68** (1987) 307-326.
- Casas-Prat, M., X.L. Wang, Projections of extreme ocean waves in the Arctic and potential implications for coastal inundation and erosion. *J. Geophys. Res. Oceans*, **125** (2020), doi: 10.1029/2019JC015745, 18pp.

- Chawla, A., H.L. Tolman, Obstruction grids for spectral wave models, *Ocean Modelling* **22** (2008) 12-25.
- Hardy, T.A., L.B. Mason, J.D. McConochie, A wave model for the Great Barrier Reef, *Ocean Engineering*, **28** (2000) 45-70.
- Hou, F., Z. Gao, J.G. Li, F. Yu, An efficient algorithm for generating a spherical multiple-cell grid. *Acta Oceanologica Sinica*, **41(5)** (2022) 41-50. doi: 10.1007/s13131-021-1947-3.
- Leonard, B.P., The ULTIMATE conservative difference scheme applied to unsteady one-dimensional advection. *Computer Methods Appl. Mech. Eng.*, **88** (1991) 17-74.
- Leonard, B.P., A.P. Lock, M.K. MacVean, Conservative explicit unrestricted-time-step multi-dimensional constancy-preserving advection schemes. *Mon. Wea. Rev.*, **124** (1996), 2588-2606.
- Li, J.G., Upstream non-oscillatory advection schemes, *Mon. Wea. Rev.*, **136** (2008) 4709-4729.
- Li, J.G., Global transport on a spherical multiple-cell grid, *Mon. Wea. Rev.*, **139** (2011) 1536-1555.
- Li, J.G., Propagation of Ocean Surface Waves on a Spherical Multiple-Cell Grid, *J. Comput. Phys.*, **231** (2012) 8262-8277.
- Li, J.G., Ocean surface waves in an ice-free Arctic Ocean. *Ocean Dynamics*, **66** (2016) 989-1004.
- Li, J.G., An efficient multi-resolution grid for global models and coupled systems. *Adv. Sci. Res.*, **16** (2019), 137-142. doi: 10.5194/asr-16-137-2019
- Li, J.G., A. Saulter, Unified global and regional wave model on a multi-resolution grid. *Ocean Dynamics*, **64** (2014) 1657-1670.
- Li, J., R. Li, Y. Ding, Y. Ma, Modelled Stokes drift in the marginal ice zones of the Arctic Ocean. *Ocean Dynamics*, **71** (2021), 509-525.
- Rasch, P.J., Conservative shape-preserving two-dimensional transport on a spherical reduced grid. *Mon. Wea. Rev.* **122** (1994) 1337-1350.
- Roe, P.L., Large scale computations in fluid mechanics, in: E. Engquist, S. Osher, R.J.C. Sommerville (Eds.), *Lectures in Applied Mathematics*, **22** (1985) 163-193.
- Tolman, H.L., A third-generation model for wind waves on slowly varying unsteady and inhomogeneous depths and currents. *J. Phys. Oceanogr.* **21** (1991) 782-792.
- Tolman, H.L., Alleviating the Garden Sprinkler Effect in wind wave models, *Ocean Modelling*, **4** (2002) 269-289.
- Tolman, H.L., Treatment of unresolved islands and ice in wind wave models, *Ocean Modelling*, **5** (2003) 219-231.
- Tolman, H.L., A mosaic approach to wind wave modeling. *Ocean Modelling*, **25** (2008) 35-47.
- Tolman, H.L., B. Balasubramaniyan, L.D. Burroughs, D.V. Chalikov, Y.Y. Chao, H.S. Chen, V.M. Gerald, Development and implementation of wind-generated ocean surface wave models at NCEP, *Weather and Forecasting*, **17** (2002) 311-333.
- WAMDI group, The WAM model - a third generation ocean wave prediction model, *J. Phys. Oceanogr.* **18** (1988) 1775-1810.
- WISE Group, L. Cavaleri, J.-H.G.M. Alves, F. Ardhuin, A. Babanin, M. Banner, K. Belibassakis, M. Benoit, M. Donelan, J. Groeneweg, T.H.C. Herbers, P. Hwang, P.A.E.M. Janssen, T. Janssen, I.V. Lavrenov, R. Magne, J. Monbaliu, M. Onorato, V. Polnikov, D. Resio, W.E. Rogers, A. Sheremet, J. McKee Smith, H.L. Tolman, G. van Vledder, J. Wolf, I. Young, Wave modelling - the state of the art. *Progress Oceanogr.* **75** (2007) 603-674.
- WAVEWATCH III® Development Group (WW3DG), *User manual and system documentation of WAVEWATCH III® V6.07*. Tech. Note 333 (2016), NOAA/NWS/NCEP/MMAB, College Park, MD, USA, 465 pp. + Appendices.
- Zieger, S., D. Greenslade, Bureau Research Report No 51 (2021) 74 pp. available online at <http://www.bom.gov.au/research/publications/researchreports/BRR-051.pdf>